New York University
A private university in the public service

Neuromagnetism Laboratory
Departments of Physics and Psychology
and Center for Neural Science

FINAL TECHNICAL REPORT

Neuromagnetic Investigations of Cortical Regions Underlying Short-Term Memory

AFOSR-91-0401

1 July 1991 - 30 June 1992

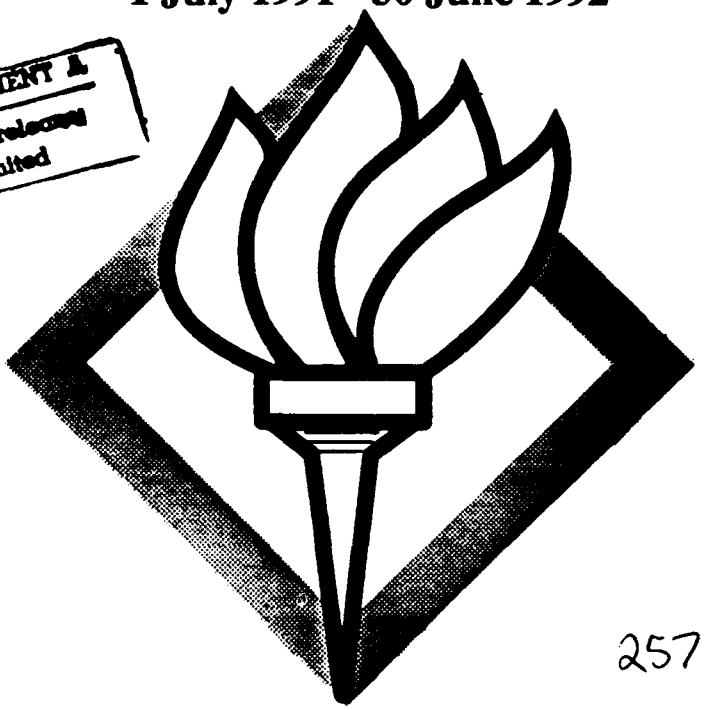

Samuel J. Williamson and Lloyd Kaufman
Principal Investigators

Prepared for:

Dr. John F. Tangney
Directorate of Life Sciences
Air Force Office of Scientific Research
Bolling AFB, DC 20332

Approved by:

Samuel J. Williamson

Lloyd Kaufman

Unclassified

SECURITY CLASSIFICATION OF THIS PAGE

REPORT DOCUMENTATION PAGE

Form Approved OMB No. 0704-0188

1a. REPORT SECURITY CLASSIFICATION Unclassified	1b. RESTRICTIVE MARKINGS
2a. SECURITY CLASSIFICATION AUTHORITY	3. DISTRIBUTION / AVAILABILITY OF REPORT Approved for public release; distribution unlimited.
2b. DECLASSIFICATION / DOWNGRADING SCHEDULE	
4. PERFORMING ORGANIZATION REPORT NUMBER(S)	5. MONITORING ORGANIZATION REPORT NUMBER(S)
6a. NAME OF PERFORMING ORGANIZATION New York University 6b. OFFICE SYMBOL (If applicable)	7a. NAME OF MONITORING ORGANIZATION Air Force Office of Scientific Research
6c. ADDRESS (City, State, and ZIP Code) Department of Physics and Psychology 4 Washington Place, New York, NY 10003	7b. ADDRESS (City, State, and ZIP Code) Building 410 Bolling AFB, DC 20332-6558
8a. NAME OF FUNDING / SPONSORING ORGANIZATION AFOSR 8b. OFFICE SYMBOL (If applicable) NL	9. PROCUREMENT INSTRUMENT IDENTIFICATION NUMBER AFOSR-91-0401
8c. ADDRESS (City, State, and ZIP Code) Building 410 Bolling AFB, DC 20332-6558	10. SOURCE OF FUNDING NUMBERS PROGRAM ELEMENT NO. 61102F; PROJECT NO. 2313; TASK NO. A4; WORK UNIT ACCESSION NO.

11. TITLE (Include Security Classification)
Neuromagnetic Investigations of Cortical Regions Underlying Short-Term Memory

12. PERSONAL AUTHOR(S)
Samuel J. Williamson and Lloyd Kaufman

13a. TYPE OF REPORT	13b. TIME COVERED	14. DATE OF REPORT (Year, Month, Day)	15. PAGE COUNT
Final	FROM 910701 TO 920630	920818	44

16. SUPPLEMENTARY NOTATION

17. COSATI CODES		
FIELD	GROUP	SUB-GROUP

18. SUBJECT TERMS (Continue on reverse if necessary and identify by block number)
Mental imagery of a target, visual cortex participation, alpha rhythm suppression, localization of cortical activity, magnetic power inverse solution, sensory memory, decay of auditory memory, central tendancy.

19. ABSTRACT (Continue on reverse if necessary and identify by block number)

Spontaneous neuronal activity of the brain within the alpha frequency bandwidth is found to be suppressed in visual cortex when comparing a rotated, and possibly inverted object with an object previously seen to determine whether they are identical. Moreover, the pattern of suppression adjusts to task demands. Thus, visual cortex participates in the processes of mental imagery. A mathematical solution for the magnetic inverse problem has been developed to determine the locations of alpha suppression within the brain based on magnetic field measurements of the magnetic field power across the scalp. Behavioral studies of a person's loss of memory for the loudness of a tone can be characterized by a decaying exponential dependence on time. The characteristic lifetime is found to match to within 0.2 sec the individual's lifetime for the decay of the neuronal activation trace in primary cortex, determined neuromagnetically.

20. DISTRIBUTION / AVAILABILITY OF ABSTRACT	21. ABSTRACT SECURITY CLASSIFICATION
☒ UNCLASSIFIED/UNLIMITED ☐ SAME AS RPT. ☐ DTIC USERS	Unclassified
22a. NAME OF RESPONSIBLE INDIVIDUAL Dr. John F. Tangney	22b. TELEPHONE (Include Area Code) 202/767-5021
	22c. OFFICE SYMBOL NL

DD Form 1473, JUN 86 Previous editions are obsolete. SECURITY CLASSIFICATION OF THIS PAGE
Unclassified

24 AUG 1992

Contents

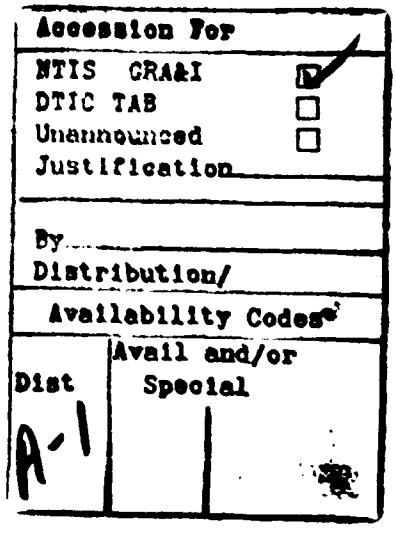

1 Summary

This report, which is submitted in accord with the requirements of Contract AFOSR-91-0401 between Air Force Office of Scientific Research and New York University, summarizes the scientific progress made during the year of grant support from 1 July 1991 to 30 June 1992.

The goal of this research is to establish the extent to which magnetic and electric measurements of brain activity provide objective measures for human cognitive functions. Two types of studies were undertaken. One focuses on the the visual system and its participation in the manipulation of mental images. We find direct relationships between the duration of suppression of spontaneous neuronal activity of visual areas of the brain and the reaction time of an individual in recognizing whether a rotated, and possibly inverted, target matches a previously seen memory figure. Moreover, the spatial pattern of suppression changes with the difficulty of the task. These findings indicate that visual areas of the brain participate in the manipulation of mental images, and that appropriate magnetic and electric measurements can indicate the sequence of activity that is called into play for specific aspects of the task.

We also made progress in further developing the minimum-norm least-squares inverse ("MNLS inverse") that we conceived for obtaining the distribution of neuronal activity within the brain from measurements of the magnetic field pattern across the scalp. The original formulation was successfully extended to provide the inverse solution for measurements of magnetic field power across the scalp, to provide a best estimate for the distribution of neuronal current power across the cerebral cortex and subcortical areas. The overall goal of this development is to enhance the specificity of neuromagnetic measurements so that measured signals can be associated with precise anatomical regions of the brain, even if activities in many diverse regions contribute to the observed magnetic signals.

A third study was carried out to provide a quantitative characterization for the duration of auditory sensory memory. Recently we established that neuromagnetic studies provide a measure for the duration of the cortical activation traces established in the auditory sensory areas of the brain in response to a sound. By carrying out appropriate behavioral studies, we have now shown a direct relationship between the lifetime of this trace in primary auditory cortex and the duration of a person's memory for the loudness of a sound. This work establishes the feasibility for noninvasive characterization of dynamical aspects of memory processes in all the human sensory systems.

2 Highlights

Here are listed the highlights of the research findings during the past year of support:

- Using the paradigm of Cooper and Shepard, the duration of suppression of spontaneous cortical activity within the alpha bandwidth over the occipital scalp for each of 6 subjects was found to match closely the subject's reaction time. This demonstrates that suppression is a reliable measure of the time for the brain to complete the comparison of probe with target.

- Suppression duration and reaction time both vary linearly with rotation angle for each subject. This finding supports the popular conjecture that a subject rotates the image of the memory figure to compare it with the target. The linear variation provides physiological evidence that rotation is carried out at a uniform rate. Suppression of spontaneous activity is not merely the result of changing levels of arousal or attention, and cannot be ascribed to differences among physical stimuli.

- The spatial pattern of suppression indicates that both visual cortex and visual areas in the parieto-occipital sulcus and neighboring parietal areas participate in the mental imagery task. This is the first direct evidence that visual cortex participates in the process of rotating the memory figure to compare with the target.

- When the target is rotated by a large angle so that the match to the memory figure is difficult, additional suppression is observed over the left parietal area. Thus by non-invasive measures, it is possible to detect when additional mental resources are called to participate in such a task.

- The mathematical "MNLS inverse" solution that we developed for neuromagnetic applications, partly with AFOSR support during the past 3 years, provides a method for computing the distribution of cortical activity from measurements of the magnetic field pattern across the scalp without recourse to explicit source models, such as a set of current dipoles. This has been extended successfully to deal with magnetic field power measurements for characterizing the the cortical distribution of spontaneous rhythmic activity. This is the first time an inverse has been developed for dealing with field (or potential) mean power.

- By comparing this extended MNLS inverse with and without the presence of alpha-band suppression, it is possible to deduce the spatial distribution of cortical areas where *suppression* of spontaneous rhythms takes place. This representation provides a functional image of the brain, revealing the evolving pattern of cortical participation in sensory or cognitive tasks, It is the magnetic source image counterpart for the well-known PET and functional MRI representations.

- In auditory studies, we discovered several characteristics of auditory evoked responses that are indicative of sensory memory. Habituation of the response can be understood in terms of a cortical activation trace that decays exponentially in time as $Ae^{-t/\tau}$, where A is the amplitude of the trace and τ is a parameter that characterizes its lifetime. We have

proposed that this relationship describes the effect of the decay of the cortical activation trace: The strength of an observed sensory-evoked response is a measure of the charge displacement required to fully activate the trace. If stimuli are presented rapidly compared with the time interval τ, there is little time for decay of the trace and the response strength is weak.

- Neuromagnetic studies of 4 subjects show a broad range of lifetimes, with τ ranging from 0.8 to 3.4 sec for the primary auditory cortex. This broad range indicates that neuromagnetic measurements may provide a useful measure of dynamical aspects of human auditory physiology which vary markedly across individuals.

- Behavioral studies on the same 4 subjects establish that auditory memory for the loudness of a tone decays with time, if in a two-alternative, forced-choice paradigm the probe tones have an average loudness that differs from that of the standard ("central tendancy").

- The evolution of each of the 4 subject's loudness judgements for various time delays t following a standard tone is well-described by a decaying exponential relationship: $De^{-t/\tau}$, where D and τ are fitting parameters. The values of τ vary considerably across subjects.

- Values of the lifetime τ obtained for each of the 4 subjects from these behavioral studies are identical with the values obtained on the same respective subjects from neuromagnetic studies. Over the range from 0.8 to 3.4 s the greatest deviation between behavioral and physiological measures is only 0.2 s.

- From the preceding evidence we conclude that primary auditory cortex supports auditory sensory memory for the loudness of a tone. The decay of the activation trace is accompanied by decay of the sensory memory for attributes of a sound, with a person's judgement depending more on long-term memory as the trace decays.

- The standard deviation describing the scatter in loudness match in the behavioral measurements is found to be independent of delay following presentation of the standard tone. We interpret this as indicating the subject is just as subjectively "certain" of his judgement, even when accuracy deteriorates with delay as judgement tends toward the mean loudness of longer-term experience (central tendancy).

3 Publications

This section lists reports of scientific and technical research carried out during the past year.

[1] C. M. Michel, L. Kaufman, and S. J. Williamson. Effects of a mental rotation task on the suppression duration of EEG and MEG occipital alpha rhythm. in preparation, 1992.

[2] L. Kaufman, S.J. Williamson, and J.Z. Wang. On the power of spontaneous brain activity. *IEEE Eng. Med. & Bio. Soc.*, submitted, 1992.

[3] Z.-L. Lü, S. J. Williamson, and L. Kaufman. Human auditory primary and association cortex have differing lifetimes for activation traces. *Brain Res.*, 527:236–241, 1992.

[4] Z.-L. Lü, S. J. Williamson, and L. Kaufman. Physiological measurements predict the lifetime for human human auditory memory of a tone. submited, 1992.

[5] J.-Z. Wang, S. J. Williamson, and L. Kaufman. Magnetic source images determined by a lead-field analysis: the unique minimum-norm least-squares estimation. *IEEE Trans. Biomed. Engr.*, 39:665–675, 1992.

[6] J.-Z. Wang, L. Kaufman, and S. J. Williamson. Imaging regional changes in the spontaneous activity of the brain: an extension of the unique minimum-norm least-squares estimate. *Electroenceph. Clin. Neurophysiol., in press*, 1992.

[7] J.-Z. Wang. Minimun-norm least-squares estimation, unique magnetic source images for a spherical model head.

[8] A.C. Bruno and S.J. Williamson. Representations of isocontours on a spherical head. *IEEE Eng. Med. & Bio. Soc., accepted*, 1992.

4 Personnel

4.1 Faculty

Lloyd Kaufman, Ph.D., Professor of Psychology and Neural Science, Adjunct Professor of Physiology and Biophysics.

Samuel J. Williamson, Sc.D., University Professor, Professor of Physics and Neural Science, Adjunct Professor of Physiology and Biophysics.

4.2 Collaborating Faculty

Murray Glanzer, Ph.D., Professor of Psychology

4.3 Research Scientists

Jia-Zhu Wang, Ph.D., Associate Research Scientist (Physics)

4.4 Collaborating Researcher

Christoph Michel, Ph.D., Research Assistant, Neurological Clinic, University Hospital of Zürich, Switzerland

4.5 Graduate Research Assistants

Daniel Karron, Ph.D. student, Department of Applied Science (not supported by AFOSR)

Zhong-Lin Lü, Ph.D. student, Department of Physics

Xiao-Lin, Ph.D. student, Department of Physics

4.6 Undergraduate Students

Divya Chander, Harvard University, Hughes Summer Scholar Research Project, 1991.

Elena Vitale, New York University, Hughes Summer Scholar Research Project, 1991.

Harmony Reynolds, New York University, Department of Physics, 1992

4.7 Degrees Awarded

Bruce Luber, Ph.D. in Psychology, "Neuromagnetic Effects of Visual Spatial Attention in Discrimination Tasks", Fall, 1991.

Yael Cycowicz, Ph.D. in Psychology, "Verbal and Imaging Tasks Have Different Effects on Spontaneous Activity of Cerebral Cortex", Fall, 1991.

Zhong-Lin Lũ, Ph.D. in Physics, "Neuromagnetic Investigations of Spontaneous and Sensory-Evoked Activity of Human Cerebral Cortex", Spring, 1992.

5 Interactions with Other Groups

S.J. Williamson was Chairman of the Advisory Committee for the 8th International Conference on Biomagnetism, held in August 1991, and he was a member of the Program Committee. He is a member of the Publications Committee and of the Editorial Board of *Biophysical Journal.*

L. Kaufman was an invited speaker at the 8th International Conference on Biomagnetism. He is a member of the Working Group on Advanced Technology in Cognitive Neuroscience of the National Research Council, a member of the Research Advisory Board of the New York Association for the Blind, and a member of the Briefing Panel on Imaging Biological Events of the Institute of Medicine, National Academy of Science.

5.1 Invited Talks given by Members of the Laboratory

Aug 4 "Advantages and Limitations of Magnetic Source Imaging." (SJW) 3rd Congress of the International Society for Brain Electromagnetic Topography, Toronto, Canada, July 29 - August 1.

Oct 25 "Human Auditory Primary and Association Cortex have Differing Lifetimes for Activation Traces." (SJW) Körber Foundation Symposium, Helsinki University of Technology, October 24-25.

Nov 1 "Magnetic Source Imaging of Human Brain Functions " (SJW) Advances in Magnetic Imaging in Medicine. A Symposium Honoring Richard B. Mazess, Department of Medical Physics, University of Wisconsin, Madison, WI.

Nov 20 "Magnetic Measures of Activity in Auditory Cortex." (SJW) Symposium on "Objective Methods for Hearing Assessment", New York Academy of Medicine, New York City, sponsored by IEEE Sections on Biomedical Engineering and Otolaryncology and the New York State Section, Engineering in Medicine and Biology Society of the Institute of Electrical and Electronic Engineers.

Nov 21 "Magnetic Source Imaging of the Human Brain." (SJW) Colloquium, Department of Physics, University of Florida, Gainesville, FL.

Dec 6 "Magnetic Source Imaging of the Human Brain." (SJW) Keynote address at the Inaugural Symposium celebrating the opening of the Superconducting Sensor Laboratory, sponsored by the Ministry of International Trade and Industry, Tokyo, Japan.

Dec 11 "Magnetic Source Imaging of the Human Brain." (SJW) Margaret and Herman Sokal Faculty Award in the Sciences, NYU.

Feb 24 "Dynamic Proceses of the Human Brain: Lifetimes of Sensory Memory and (SJW) the Time Required to Scan Memory", Magnetoencehpalography Workshop, Centre National de la Recherch Scientifique, Centre de Formation Permanente du C.N.R.S., Gif sur Yvette, France

Feb 24 "Magnetic Source Imaging of the Human Brain", (SJW) Seminar, Ecole Normal Superieur, Paris, France

April 11 "Magnetic Source Imaging of the Human Brain", (SJW) Spring Meeting, New York State Section of the American Physical Society, Syracuse, New York

June 10 "Magnetic Source Images for Distributed Cortical Activity", (SJW) Plenary Symposium, 3rd International Congress on Brain Electromagnetic Topography, Amsterdam, The Netherlands, June 9-12, 1992.

June 16 "Progress in the Development of Neuromagnetic Techniques for Producing (SJW) Magnetic Source Images", Vacuumschmelze Corporation, Hanau, Germany.

June 17 "Magnetic Source Imaging: A Physiological Approach to Understanding (SJW) Sensory Memory in the Human Auditory Cortex", Physiologisches Kolloquium, Physiologisches-Institut, Klinikum der Justus-Liebig-Universität Geissen, Gießen, Germany.

5.2 Contributed Presentations

Latent Neuronal Activity in Human Auditory Cortex. (Slide presentation)
Z.L. Lü, S.J. Williamson, and L. Kaufman
Society for Neuroscience Annual Meeting, New Orleans, LA, Nov. 10-15, 1991.

"Lifetimes of Activation Traces in Human Auditory Cortex"
S.J. Williamson
Seventeenth Annual Interdisciplinary Conference
Teton Village, Jackson, Wyoming, Jan 15, 1992.

"A Unique Solution for the Inverse Problem in Magnetic Source Imaging"
J.Z. Wang, S.J Williamson, and L. Kaufman
American Physical Society March Meeting, Indianapolis, Indiana,
March 15-20, 1992.
Bull. American Physical Society 37: 755 (1992).

"Visualization of Comprehensive Source Searching Procedure in Magnetic Source Imaging (MSI)"
Daniel Karron, Zhong-Lin Lu, and Samuel J. Williamson
IEEE Conference on Visualization in Biomedical Computing, Florida,
1992.

"Unique Inverse Solution to Obtain Magnetic Source Images of Alpha Power Suppression"
Jia-Zhu Wang, Lloyd Kaufman, and Samuel J. Williamson
Tenth International Conference on Event-Related Potentials of the Brain
(EPIC-X), Eger Hungary, June 1-5, 1992.

"Neuromagnetic Measures for the Decay of Auditory Sensory Memories"
Samuel J. Williamsin, Zhong-Lin Lü, and Lloyd Kaufman
Tenth International Conference on Event-Related Potentials of the Brain
(EPIC-X), Eger Hungary, June 1-5, 1992.

6 Inventions and Patent Disclosures

The development of the extended minimum-norm least-squares (MNLS) estimation for obtaining a unique solution for the magnetic inverse problem for measurements of field power was deemed of possible interest for protection. NYU provided a small grant to help in its further development. The possibility of obtaining a patent is presently under consideration by the Office of Industrial Liaison at NYU.

7 Visual Imagery: Mental Rotation

7.1 Summary

Mental rotation is of importance in cognitive psychology for two principal reasons. It is the clearest example of a cognitive process that is isomorphic with the physical process being represented, *viz.* a physical rotation of an object. The primary evidence for this is that the time needed to complete a mental rotation is proportional to the angle of rotation. It is also a clear example of the kind of visualization used by engineers, artists, and pilots to simulate the effects of real displacements and manipulations of objects in the physical world [1]. We test the hypothesis that neuronal activity of visual cortex and visual association areas of the brain provide objective measures for the involvement of specific areas of the brain in mental imagery tasks. In particular, this study provides evidence that electric and magnetic measurements of neuronal activity reveal different stages of processing, dependent on the difficulty of the task.

We find that the strength and spatial distribution of spontaneous rhythmic activity of cerebral cortex are altered during a task requiring mental rotation, and that behavioral indices of mental rotation coincide with these changes in cortical activity. In this study, the duration of suppression of spontaneous neuronal activity in the alpha bandwidth is found to vary in the same way as reaction time when a rotated visual target is compared with a memory figure previously seen to determine whether or not it matches. This functional relationship provides a direct connection between objective "physiological" measures of brain function and psychophysical measures of behavior. It provides strong support for the notion that mental imagery is served by both visual cortex and allied association areas.

This research was carried out in collaboration with Dr. Christoph M. Michel of the Department of Neurology, University Hospital, Zürich, Switzerland. His participation was supported by the Swiss National Science Foundation.

We investigated the duration of alpha suppression over the occipital scalp during a classic visual mental rotation task. Measurements on 6 subjects were taken at 9 EEG electrode positions and 30 magnetic sensor positions. Two identical alphanumeric characters were visually presented, the first in the upright position (memory figure) and the second tilted at one of 8 possible angles between 0 and 360 degrees (target figure). Subjects pressed one of two buttons to indicate whether the target figure was presented correctly or as a mirror reflection. The results show a clear relationship between the increase in reaction time and duration of alpha suppression as task difficulty is increased. Both reaction time and suppression duration increase with increasing rotation angle in all subjects and all recorded EEG and MEG positions. The spatial pattern of the alpha activity reveals small but significant enhancement of the alpha suppression in the parietal region in the early period after the presentation of the target figure as compared with the same period after the prior presentation of the memory figure. During the latter portion of the suppression period following the target there is additional suppression of neuronal activity in the right parietal area when the targets are rotated by a large angle as compared to non-rotated targets. The data indicate that the duration and the pattern of neuronal alpha-band activity in the parieto-occipital region adjusts to the demands that are required to complete a mental rotation task.

7.2 Background

The question whether the visual system is involved in mental imagery has long been debated (Golla et al. [2]; Shepard and Meltzer [3]; Shepard and Cooper [4]; Kosslyn [5]; Farah [6]; Anderson [7]). Shepard and his colleagues (Shepard and Metzler [3]; Cooper and Shepard [8]; Finke and Shepard [9]) concluded from extensive behavioral experiments based on mental rotation tasks that mental imagery involves the same neural circuits as those employed in processing real visual images. For instance, the interstimulus interval (ISI) needed to produce optimum stoboscopic rotation of a form increases at the same rate as does the time to mentally rotate the same form. This correspondance suggests that the machinery of the visual system is involved in imagery tasks. However, alternative theories are not lacking. For example, Pylyshyn [10] argued that the same increase in time required for mental rotation with greater angles could be accounted for if more time is required to test hypotheses in working memory about abstract features of these same visual objects.

One way toward resolving such issues is to establish directly whether the visual areas of the brain are actually active when subjects mentally rotate imagined objects. However, even such a finding would be insufficient to establish a "visual machinery" theory of mental rotation. Other areas not normally involved in visual functions may be recruited in mental rotation and, by the same token, visual areas may serve some roles in non-sensory inferential processes. Nevertheless, activity of the visual areas of cortex is a necessary condition if the visual machinery theory is to be confirmed. In this research we tested the hypothesis that activity of visual areas of the brain is altered during mental rotation, and that behavioral indices of mental rotation time coincide with these changes in cortical activity.

There is some precedent for this. For example, Farah and her colleagues employed the event-related potential (ERP) to determine whether visual areas are differentially affected by the formation of mental images. Farah [11] and Farah et al. [12] recorded the ERPs to visual stimuli that were or were not preceded by an acoustic cue. They demonstrated that mentally imaging a stimulus before it was presented increased detection accuracy and enhanced the amplitude of the first negative event-related component (with 170 ms latency) over the temporo-occipital recording sites. This effect on early modality-specific stages of information processing led Farah et al. [12] to conclude that mental imagery is accompanied by changes in the visual system and these are correlated with the content of the image.

While these results suggest that visual cortex becomes differentially active if a person forms mental images of objects about to be seen, similar enhancements of the same components of the ERP accompany selectively attending to objects in visual space (Mangun and Hillyard [13]). Recently, Peronnet and Farah [14] have recorded broad, late components (400-1700 ms) of the ERP with electrodes along the midline that exhibit 10-20% enhancements in proportion to the angle of rotation in a matching paradigm. However, here again there is no direct evidence to separate more generalized attentional effects from processes that are specific to mental imagery.

Therefore, it is of value to conduct an experiment in which the time or effort involved in a mental imagery task is available for comparison with the duration or intensity of a change in local brain activity. Such an experiment was recently described by Ruchkin et al. (1991) [15] and Peronnet and Farah [14] in which event related slow wave potentials were studied for visual stimuli with easy and with difficult rotation angles. They found that slow wave

negativity at centro-parietal sites increased with increasing rotation difficulty, which might suggest the involvement of visual cortical areas in mental rotation. However, the durations (latencies) of these slow waves do not correspond to the times required for mental rotation, although enhanced amplitude with increased rotation difficulty was observed. Therefore, these differences in amplitude of slow waves do not constitute direct evidence that the time course of activity in visual or non-visual areas of cortex is related to mental imagery, as reflected in the mental rotation task.

On the other hand, there is increasing evidence that the amplitude of spontaneous cortical rhythm are modulated over specific anatomical areas of the scalp when a subject is engaged in sensory, motor and cognitive tasks. For instance, activity in the alpha frequency range (8-12 Hz) is suppressed over posterior areas after visual stimulation (Berger [16]; Kaufman and Locker [17]; Pfurtscheller [18]) and before and after eye movements (Lehmann [19]). Beta rhythm (18-30 Hz) is suppressed in central regions in association with hand movements (Jasper and Andrews [20]; Pfurtscheller [21]; and central mu rhythm (7-13 Hz) is bilateral symmetrically suppressed during planning and execution of unilateral movements (Pfurtscheller and Aranibar [22]). Extensive studies carried out by Pfurtscheller and collaborators revealed reduction in alpha band power ("desynchronization" in their terminology) whose strength and spatial distribution was related to specific sensory-motor (Pfurtscheller and Aranibar [22]; Pfurtscheller and Klimesch [23]; Klimesch et al. [24]).

Besides spatially selective alpha suppression, Kaufman et al. [25] [26] demonstrated with magnetoencephalographic recordings, that the duration of alpha suppression is closely related to specific cognitive functions. In a task where subjects were engaged in comparing the image of an abstract figure with a memory set of three figures previously seen, the duration of parieto-occipital alpha suppression was comparable to the reaction time indicating whether there was a match or not. Moreover, the suppression of alpha power was enhanced over areas along the midline of the occipital scalp. This corresponds to neuronal sources lying within the visual cortex. Suppression was also observed in the same time window for what may be a particularly strong source of alpha rhythm – the parieto-occipital sulcus (Williamson and Kaufman [27]; Williamson et al. [28]), the posterior bank of which is a visual area. Together with the temporal window within which suppression is observed, this provides strong evidence that the visual cortex participates in the process of mental imagery. However, the case would be more compelling if the duration of a cognitive task were manipulated by increasing the task difficulty, and as a result a strong positive covariation were found between reaction time to task completion and the alpha suppression duration.

This was the case for scanning short-term memory for a previously heard musical tone (Kaufman et al. [29]). A Sternberg task was carried out in which subjects determined whether a tone matched one just heard in a memory set. There was a significant positive correlation between the duration of alpha suppression measured over the right temporal area and the number of tones in the memory set. Moreover, the spatial pattern of suppression over the scalp correlated with the pattern for the magnetic N100 response of primary auditory cortex. This indicates that the source of the suppressed rhythm includes the primary auditory cortex. Direct evidence for spontaneous rhythmic activity at about 10 Hz in auditory cortex was recently reported by Tiihonen et al. [30] from magnetic source images. Thus there is converging evidence that spontaneous rhythms are produced by many cortical areas, and when a particular area becomes involved in a sensory or cognitive process the corresponding

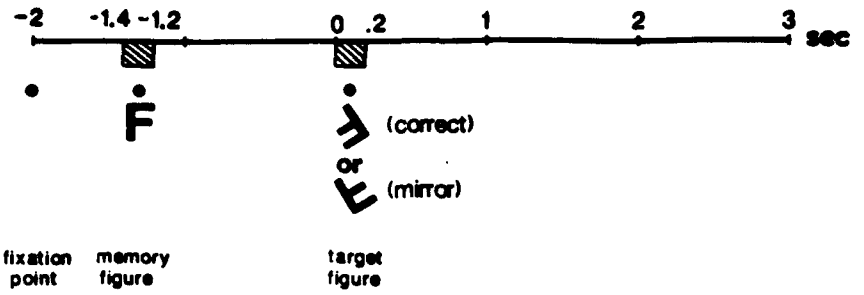

Figure 1: Representation of the time sequence of events for a single 5-s epoch. The time origin indicates the onset of the target figure. The memory figure appears between -1.4 s and -1.2 s, and the rotated target figure (same letter) appears between 0 and 0.2 s. A fixation point on top of the figures is continuously presented throughout the period between -2 s and 0.2 s. This example shows a 150 deg rotated target figure. The target figure was randomly presented either in correct orientation, or as the mirror reflected image.

rhythm is suppressed. This provides opportunities for a broad range of studies of cognitive functions, with the advantage that the signal being monitored is considerably stronger than that of event-related fields or potentials.

The present study was carried out to test a central issue that was unanswered by previous studies: whether the temporal duration of alpha suppression over the visual cortex correlates with the behavioral measure of reaction time as the time required to complete a mental rotation task is made to vary. We used the mental rotation paradigm introduced by Cooper and Shepard [8] to manipulate the neuronal processing time that presumably corresponds to the time required to perform the mental rotation task. In this task subjects are asked to discriminate normal from mirror reflected versions of alphanumeric characters when they are tilted at different angles with respect to the upright position. This well controlled and replicated task is known to produce clear correlations between the angle of tilt and reaction time, suggesting different durations of mental imagery for discrimination of target figures.

7.3 Method

Six healthy, paid volunteers (2 males and 4 females) participated in this study after giving their informed consent. Their ages ranged from 19 to 31 years. All of them were right handed and had normal, uncorrected vision. Before the actual recording sessions each subject performed at least 2 training runs of the task without recordings being made. Subjects were informed to respond as quickly as possible while trying to maintain high accuracy.

The time sequence of a single epoch is illustrated in Fig. 1. It begins with the presentation of a fixation point on a viewing screen positioned in front of the subject. This is produced from outside our magnetically shielded room by an Elektrohome video projector controlled by an Amiga 2000 computer. The memory figure in the upright position was presented under the fixation point 700 ms later. After 200 ms it was turned off while the fixation point persisted for 1.2 s on the screen. Then the target figure was presented for 200 ms duration. Subsequently the screen was darkened for 3.2 s until the fixation point for the next epoch

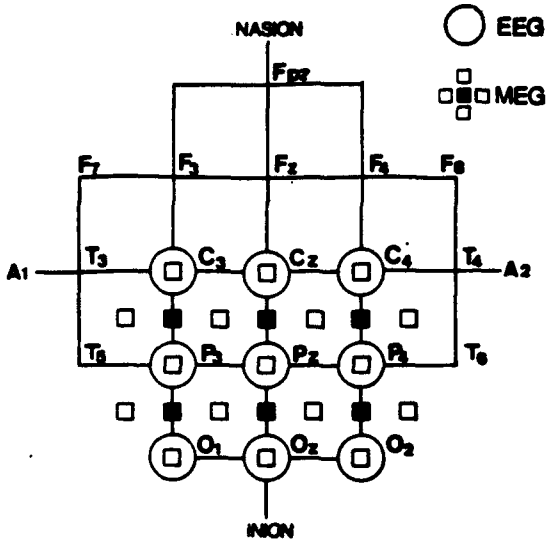

Figure 2: Positions of the 9 EEG electrodes (circles) and 30 MEG sensors (squares) with respect to the 10-20 system. Solid squares indicate the middle sensor for each placement of the 5-channel MEG probe.

was presented. Eight different figures were generated (letters C, E, F, G, L, P, S) with a font that distinguishes between upright and inverted presentation of the letters C, E, and S. The target figure was always the same as the memory figure but was tilted clockwise by a randomly selected angle from the set 0, 50, 100, 150, 210, 260, and 310 deg. In addition, each target figure was randomly chosen to be presented either normal or mirror reflected. The subject's task was to press one of two buttons with the right hand to indicate whether the target figure was normal or mirror reflected.

Multichannel measurements of both magnetic (MEG) and electric (EEG) signals were recorded over the posterior scalp. Since the two methods yield complementary information (Williamson and Kaufman [31]), the simultaneous measurements provide a more complete insight into the underlying activity. The EEG was recorded from 9 electrodes positioned over the posterior area of the scalp as shown in Fig. 2 (C3, Cz, C4, P3,Pz, P4, O1, Oz, O2 according to the 10-20 system). The electrode at Cz was used as the recording reference, and the data were recomputed to express signals relative to the average reference (Lehmann and Skrandies [32]). EEG data were bandpassed between 0.1-30 Hz.

Magnetic data were recorded with a 5-channel neuromagnetometer (Williamson et al. [33]) located within a magnetically shielded room. The probe, consisting of detection coils and SQUID sensors to which they were attached, was immersed in liquid helium within a fiberglas cryogenic vessel. The detection coils were second-order gradiometers with 1.5 cm diameter and 4 cm baseline, arranged with four sensors equally spaced on a 2 cm circle and the fifth in the center. Bandpass filters for the MEG channels were set for 0.1-50 Hz. MEG signals were recorded from 6 different probe locations, each obtained in an individual session. The sequence of positions was varied across subjects. The approximate positions

for magnetic recordings in comparison with the 9 EEG positions are illustrated in Fig. 2.

7.4 Procedure

Both EEG and MEG signals were recorded for 5 s of each epoch, starting with the presentation of the fixation point at the −2 s time point in Fig. 1. A separate trigger channel and two separate response channels as well as information about the presented stimulus (letter, angle, and type) were simultaneously recorded. The data were digitized with a sampling rate of 128 Hz and stored on computer disk for off-line analysis. Each subject participated in 6 sessions on 3 different days within less than 2 weeks. On each day, 2 experimental sessions were performed with different probe positions, separated by a rest break of 20 min. Each session consisted of 6 runs of 40 epochs each. One run lasted 3.6 min and was followed by a pause of 1 min.

Each session began with electrodes being attached to the scalp, and then the subject was comfortably positioned on a kneeling chair inside the magnetically shielded room. Torso and head were tilted forward so that they were supported by firm cushions and vacuum casts. A system of mirrors was adjusted so that the target (3 cm height) was presented in the lower visual field at a distance of 36 cm from the subject (viewing size of the figure is 4.8 deg arc).

The recording positions of the neuromagnetometer probe relative to three cardinal landmarks on the head (left and right periauricular points and nasion) of each subject was determined by standard procedures (Yamamoto et al. [34]) using the Probe Position Indicator system (Williamson and Kaufman [28]). Two receivers were stuck to a Velcro headband, and their positions were recorded relative to the three landmarks on the head to establish the head-based coordinate system. The location and orientation of the probe relative to this head-based coordinate system was determined automatically before and after each recording (PPI system, Biomagnetic Technologies Inc., San Diego, CA).

7.5 Data Analysis

Pilot studies suggested that the clearest suppression was observed within the higher alpha bandwidth of 10-12 Hz. Consequently each 5 s record of EEG and MEG recordings was bandpassed in the range 10-12 Hz (−3 db points) using a digital FIR filter with a rolloff of 48 db/octave. The filtered signals were squared and then low-pass filtered with a cutoff of 6 Hz, to provide a slowly varying envelope of the alpha rhythm's power. These power traces were averaged over the 6 runs of each session, separately for the 8 angles and the 2 conditions (correct or mirror reflected target). Only correct responses were included in the average, which left about 20 epochs to be averaged together for each run, depending on the random generator and number of correct responses. The square root of averaged power values were then taken, providing the "alpha amplitude" for each average.

The durations of alpha suppression after the memory figure, and after the target figure were computed separately. To determine the onset of suppression the program searched for the time when the average amplitude fell below 50% of the amplitude span between the preceding maximum and the following minimum. The offset of suppression was defined similarly as when the amplitude rose above 50% of the span between the minimum and the following maximum. These time marks were accepted when the amplitude exceeded the 50% threshold for at least 100 ms. The search was carried out within the time period between

−1.7 s and 0 s for the memory figure and between 0 s and 2.8 s for the target figure. Traces were then randomly displayed, without identification, on a computer monitor together with the time marks for onset and offset, and corrections were made where there were obvious miss-identifications by the computer algorithm.

While the present experiment was not designed to characterize the spatial evolution of magnetic or electric field power, it was possible to obtain some preliminary information about changes in the distribution under the sensor arrays. As a practical measure we focussed on a one-point descriptor for the spatial pattern of the alpha at each moment in time: the location of the center of gravity or *centroid* (Lehmann [35]; Michel et al. [36]). Neuronal current sources within the parieto-occipital sulcus are oriented perpendicular to the sulcus, so their field (and field-power) extrema are over the left and right ends of the sulcus. These extrema dominate the spatial pattern of alpha power. They are supplemented by activity within the parietal areas as well. Sources in visual cortex within the longitudinal fissure and calcarine sulcus produce weaker alpha field power over occipital and parietal regions.

It is assumed that a shift of the centroid location means a shift of the dominant alpha activity across the scalp. The spatial extent of the sensor array was sufficiently broad over parietal and occipital regions to indicate if the centroid shifts away from the region where alpha suppression had been dominant. The mean locations of the centroids, described by their anterior-posterior and their left-right locations were compared between different time periods by averaging the centroids over three different 500 ms time intervals: after the onset of memory figure, after the onset of the target figure, and between 500-1000 ms after the target figure. The latter two periods reflecting early and late parts of the target-induced alpha suppression.

7.6 Results

7.6.1 Reaction Time and Suppression Duration

The visual inspection of all single traces indicated that alpha rhythm was suppressed after the memory as well as after the target figure in all 9 EEG channels and all 30 MEG channels in all subjects. The interval between the memory and target figure was long enough to reestablish alpha activity before the onset of the target stimulus. The computed suppression duration had to be corrected on the basis of the inspection of the individual traces in 19.5% of all cases. In these cases, the automatic duration computation failed mainly because of low alpha amplitude at time of stimulus onset and thus a corresponding small decrease of alpha after the stimulus. There was no significant difference between the different MEG or EEG sensors. Statistical comparison of the suppression duration of the different sensors by repeated measure ANOVA's failed to show any significant differences. For further analysis the suppression duration values were averaged over all sensors, separately for each subject, each angle and each condition.

Fig. 3a (MEG) and Fig. 3b (EEG) show representative alpha amplitude traces of one subject, separately for non-rotated (mean of 0 and 360 deg) and for markedly rotated angles (mean of 150 and 210 deg). The traces are means over all 30 MEG and all 9 EEG sensors respectively. They illustrate that both EEG and MEG show stronger and prolonged suppression of alpha amplitude during the time a subject was identifying the target figure (S2) as compared to the time after the presentation of the memory figure (S1). Moreover there

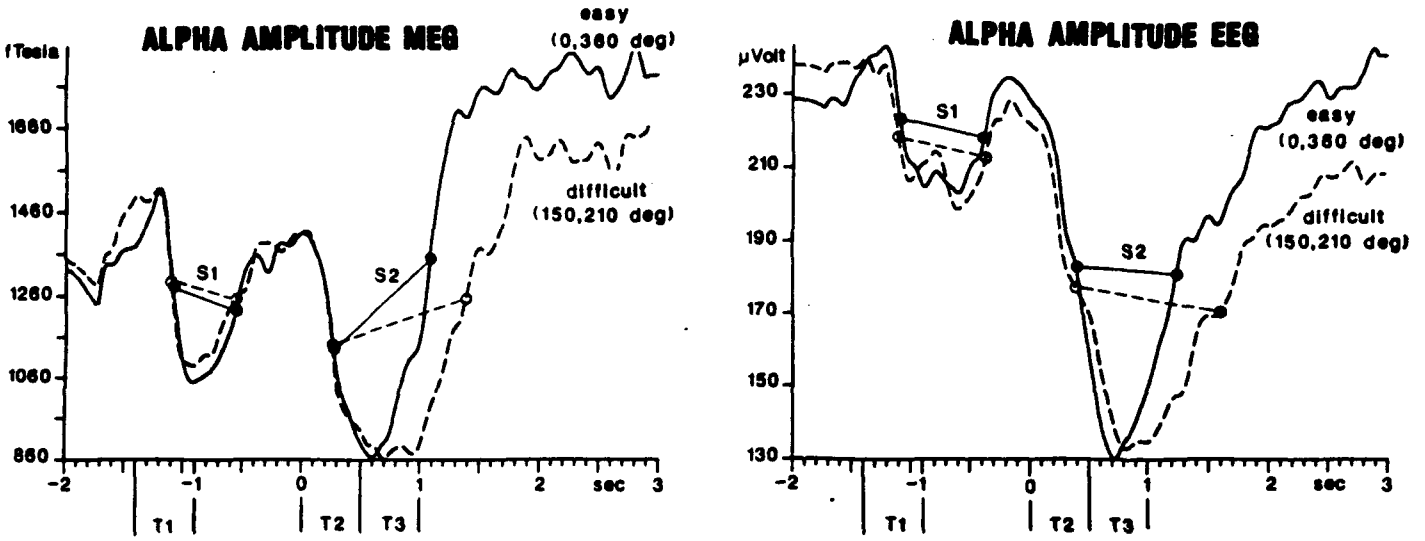

Figure 3: Five-second alpha amplitude traces of one subject as the mean over all MEG and EEG channels respectively. The time axis is the same as in Fig. 1 (the time origin indicates the onset of the target figure). Separate traces are shown for the easy angles (mean for 0 and 360 deg) and for the difficult angles (mean for 150 and 210 deg). The computed suppression duration after the memory and after the target figure for this case are indicated (S1 and S2). The time periods (T1, T2, T3) marked along the x-axis designate the epochs that were selected for averaging the centroid locations (see Fig. 7). (a) MEG alpha amplitude, averaged over all 30 sensor positions. (b) EEG alpha amplitude, averaged over all 9 electrode positions and the 6 sessions.

is evidence for longer suppression after difficult in contrast to easy rotation angles.

Fig. 4 shows the individual traces of reaction time, EEG-, and MEG suppression duration as a function of the angle of the target figure, separately for the correct and for the mirror reflected targets. Although individual differences were observed, the general trend for inverted U-shaped curves was evident, i.e. reaction time as well as suppression duration increased with increasing rotation angle. In all traces, non-rotated target stimuli (0 and 360 deg) produced faster reaction times and shorter suppression durations than strongly rotated stimuli. There was no consistent difference between reaction time and the duration of EEG- or MEG alpha suppression. The mean reaction and suppression times were different between the subjects but it did not affect the differences between easy and difficult rotation angles.

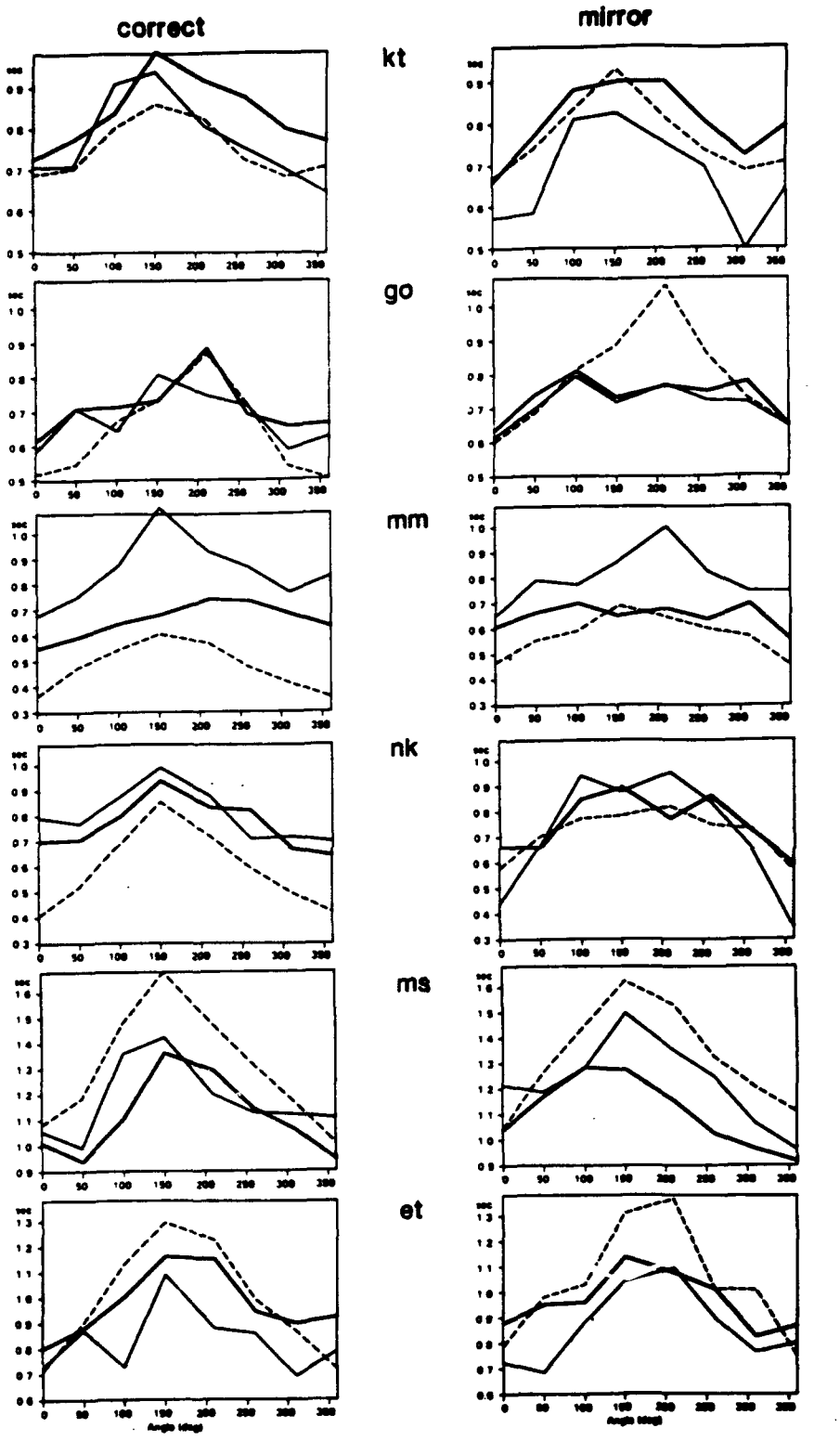

Figure 4: Individual's mean reaction time compared with MEG- and EEG suppression duration for different rotation angles of the target figures for each of 6 subjects. Separate traces are drawn for the correctly oriented (left) and for the mirror reflected (right) target figures.

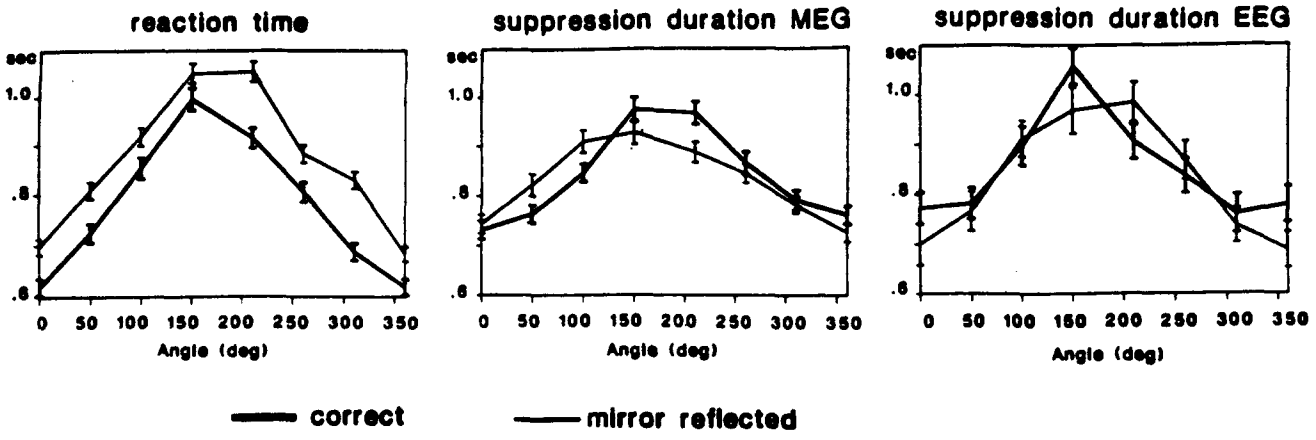

Figure 5: Mean and standard error (N = 6) of the reaction time together with MEG- and EEG suppression durations for the different rotation angles of the target figures. Separate traces are drawn for the correctly oriented and for the mirror-reflected figures.

Fig. 5 shows the mean and standard error of the reaction time and the suppression durations over the six subjects as a function of the rotation angle. These data were statistically tested for consistency over subjects by repeated measure ANOVA's with the factors "condition" (2 levels: correct and mirror) and "angles" (8 levels). It resulted in highly significant main effects of the factor "angle" [reaction time: $F(7,35) = 22.0$, $p < .001$; MEG suppression duration: $F(7,35) = 15.2$, $p < .001$; EEG suppression duration: $F(7,35) = 20.43$, $p < .001$)]. The main effect for the factor "condition" was significant for the reaction time only [$F(1,5) = 11.1$, $p = .02$] while no differences between correct and mirror reflected targets were found for the EEG and MEG suppression duration [MEG: $F(1,5) = 0.9$, EEG: $F(2,5) = 0.6$]. Clear statistical proof for the inverted U-shaped profiles were revealed by polynomial contrast analysis, where the quadratic trend was highly significant for all three variables [Reaction time: $F(1,5) = 29.8$, $p = .003$; MEG suppression duration: $F(1,5) = 51.3$, $p < .001$; EEG suppression duration: $F(1,5) = 63.1$, $p < .001$].

7.7 Spatial Features

Figure 6 illustrates EEG and MEG maps of one subject that show how the centroid is related to the field pattern. It also illustrates the main topographical distribution of alpha activity over the parieto-occipital area: Power is maximal over medial occipital sites for the EEG and over left and right lateral sites for the MEG. This is expected if the intracellular currents of dominant cortical sources are aligned approximately perpendicular to the parieto-occipital sulcus. The pattern agrees with detailed neuromagnetic studies that characterize parieto-occipital alpha rhythm in terms of a parade of cortical excitations (alphons) that are located on the walls of that sulcus [27] [28]. In addition, we may expect contributions to the

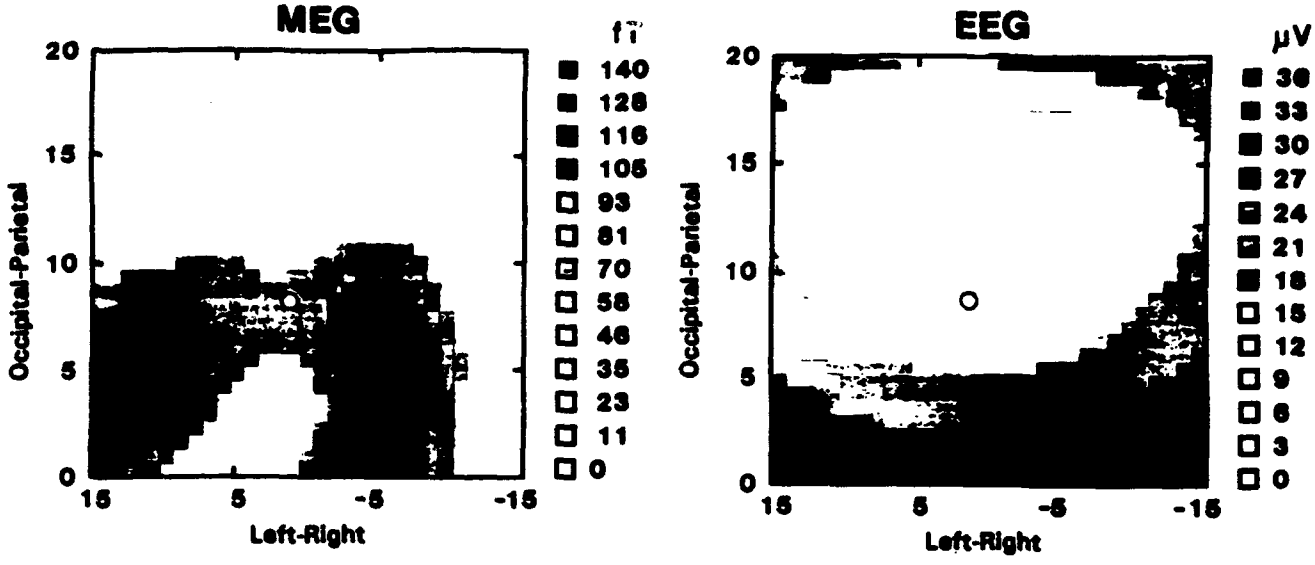

Figure 6: EEG and MEG alpha amplitude maps for one subject. The maps are means over 500 ms intervals when the target figure was rotated by 150 deg. Note the MEG patterns are oriented approximately perpendicular to the EEG patterns. The locations of the respective amplitude centroids are marked by white dots. The values on the axis are in centimeters, with the inion at the origin for the occipital-parietal axis and the midline at the origin for the left-right axis, with negative to the right.

measured field from the adjacent parietal area.

Across subjects, the average locations of the centroids of the EEG and the MEG alpha amplitudes did not differ significantly between the eight different rotation angles. That is, unlike the reaction time or suppression duration data, there were no significant ANOVA or polynomial contrast effects for field amplitudes. However, significant differences were found in the comparison of the centroid locations between the non-rotated (mean of 0 and 360 deg) and the large rotation angles (mean of 150 and 210 deg). The centroid locations of these "easy" and "difficult" conditions are shown in Fig. 7. The analysis of the late suppression period after the target (T3, between 500 and 1000 ms as defined in Fig. 3) showed a more posteriorly located MEG centroid than after the memory figure. This shift in the MEG pattern was independent of the rotation angle of the target figure. A similar shift was evident in the EEG for the easy condition.

A significant shift in the MEG centroid in the rightward direction for the difficult condition was found for the late target period T3, while a leftward shift was indicated for the easy condition. The shifts were small but they were in the same direction in all 6 subjects for the MEG centroid (Wilcoxon test: $Z = 2.2$, $p = .28$ for both angles) and in 5 of the 6 subjects for the EEG centroid ($Z = 1.99$, $p = .046$ for both angles). This shift resulted in significant differences in the comparison between the late and the early period (period T3 vs period T2) for the EEG ($Z = 1.99$, $p = .046$, 5 of 6 subjects) and for the MEG ($Z = 2.2$,

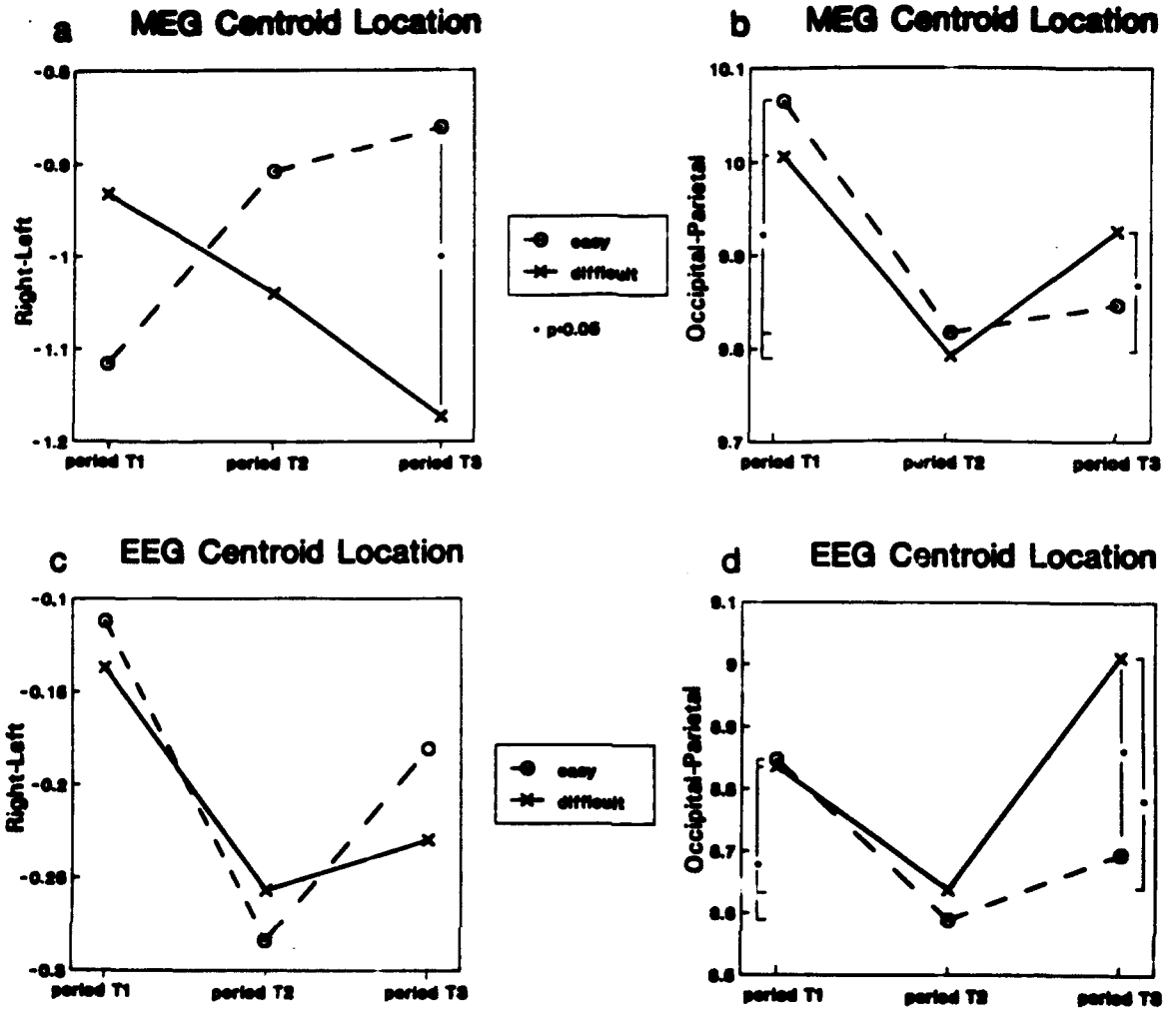

Figure 7: Location of the centroids of the MEG and the EEG field patterns, averaged over 3 different time periods: T1: 0-500 ms after onset of the memory figure; T2: 0-500 ms after onset of the target figure; and T3: 500-1000 ms after onset of the target figure. Separate traces are shown for the easy (0, 360 deg) and difficult (150, 210 deg) rotation angle of the target figures. All points are the means over six subjects. Statistically significant differences (Wilcoxon-tests) are marked by an asterisk and vertical lines. Coordinate axes are as in the preceding figure. (a) Right-Left of the centroid of the MEG field (negative is in right hemisphere). (b) Occipital-Parietal location of the centroid of the MEG field.

$p = .28$, 6 of 6 subjects). Direct differences between easy and difficult conditions within period T3 was significant for the EEG centroid ($Z = 2.2$, $p = .028$, 6 of 6 subjects). In addition, the centroid of the alpha field during this late suppression period was located more to the right for the large rotation angles as compared with the non-rotated angles. However, this difference was significant for the MEG measurement only ($Z = 1.99$, $p = .46$, 5 of 6 subjects).

7.8 Discussion

The reaction time results in this study clearly replicated the findings described by Cooper and Shepard [8]. Reaction time increased with increasing rotation of the target figure from the normal orientation. Therefore the mental rotation task clearly fulfilled our requirements to produce different response latencies for different levels of task difficulty. As proposed by Finke and Shepard [9] the present reaction time results are consistent with the notion that subjects mentally carry out a rotation of the figure back into the normal position before making an identification. Our data are consistent with a linear variation, implying that the time to re-orient the figure is proportional to the rotation angle. Since there was no difference in the reaction and suppression times between the angles from 0 to 150 deg and from 210 to 360 deg, the figures seemed to be re-oriented either in the clockwise or counter-clockwise direction, depending on the smallest angle of rotation needed to get to the upright position. The responses to the mirror reflected letters appeared to be about 50 ms longer than those to the letters with correct orientation, indicating that additional processes were required when the stimuli were mirror reflected. However, this additional amount of time was essentially independent of the rotation angle.

Both the MEG and the EEG measures showed suppression of the alpha activity after the presentation of the stimuli. Suppression was observed after presentation of the memory figure as well as the target figure. All recorded MEG and EEG channels showed this suppression of the alpha amplitude. This finding is in agreement with early EEG-reports about parieto-occipital alpha blocking after visual stimulation (Morrell [37]).

The present study has now established a clear relationship between the increase in duration of suppression of parieto-occipital alpha band neuronal activity and reaction time as task difficulty is increased in a mental rotation paradigm. Both increased by about 200 ms for greater angles of rotation in a consistent fashion for each subject. This trend was independent of the different individual's reaction times for the non-rotated targets (0 and 360 deg). Intrestingly, while the reaction time was generally longer for mirror reflected than correctly oriented target stimuli, this was not revealed by the duration of the alpha suppression. However, since the difference in the reaction time was relatively small, the absence of such an effect for the suppression duration could have been due to the uncertainty in establishing suppression onset and offset times. The accuracy in determing these physiological measures was dependent on the strength of the alpha rhythm at stimulus onset. Because cortical excitations (alphons) that produce the parade of spindles comprising the alpha rhythm have many different spectral and temporal configurations (Ilmoniemi et al. [38]), there may be none in the relevant cortical areas at the moment of interest and therefore suppression may not have been clearly observed. However, these cases were rare and alpha suppression occurred in the majority of the cases. The fact that this suppression was stronger and markedly

longer when the subject was engaged in the figure identification task, and its duration was longer when this task was made more difficult (strongly rotated figures) indicates that the region of the brain supporting this rhythm was involved in the mental rotation task. As noted earlier in a study of mental imagery in a figure matching task, sources in the visual cortex (Kaufman et al. [26]) and parieto-occipital sulcus (Williamson et al. [27]) contribute to these fields.

Although the number of sensors employed to measure the EEG and MEG activity was rather small, changes of the spatial pattern during the period of alpha suppression were observed. The analysis of the locations of the centroids of electric and magnetic field power registered by the sensors revealed small but statistically significant shifts depending on the task requirements of the stimuli (memory vs. target figure) and depending on level of difficulty for the rotation task (easy vs. difficult angle). The spatial patterns of MEG and EEG alpha signals often consist of only two extremas with opposite polarity (Williamson et al. [28]; Michel et al. [36]). The selected maps in Fig. 6 show the two extremas for the MEG and an occipital extremum for the EEG. The anterior extremum for the EEG was not captured completely in this example. For such bipolar field patterns the center of gravity of the maps approximates the 2-dimensional location on the scalp of the underlying generator. A shift of this point within the measured array indicates changes in the spatial activity pattern of the different neural populations exhibiting the spontaneous activity (Lehmann [39]; Michel et al. [36]).

In the first 500 ms after the memory and target figures, the centroid locations of both the EEG and the MEG shifted towards more occipital regions after the target figure as compared to the same period after the memory figure, independent of the time needed to identify the stimulus. This means that early suppression was stronger in the parietal region when an analysis task was required with the visual stimulus. Alpha pattern differences between the easy condition (no rotation) and difficult condition (large rotation) were found in the later period (500 - 1000 ms) after the target stimuli, where the centroids shifted towards the right (significant for the MEG) and parietal areas (significant for the EEG) when processing the targets with the difficult condition. This effect suggests additional suppression of neuronal activity in the left occipital area. Our study was not designed primarily to study hemispheric differences, and in view of the confusing literature Kosslyn [40]; Papanicolaou et al. [41]; Corballis and Sergent [42] [43]; and Servos and Peters [44]) further studies are needed to define a clear left hemispheric involvement in mental imagery. Since these spatial changes give the first evidence for local changes of alpha activity that depend on the task demands, it is clear that measurements with larger arrays of field sensors, together with the newly developed Minimum-Norm Least-Squares proceedures for obtaining inverse solutions ("MNLS inverse") for measurements of the distribution of magnetic field power (Wang et al. [45]), will make it possible to map in detail the evolution of the activity pattern associated with alpha suppression. The high temporal correlation between behavioral measures and alpha suppression make this physiological measure a clear candidate for studies of brain processes that serve cognitive functions.

7.9 Acknowledgment

We thank Divya Chander for her help in conducting the experiment, Dr. Y.M. Cycowicz and Dr. Z.L. Lü for their technical advice, Dr. J.-Z. Wang for computer assistance, and Dr. D. Lehmann for his helpful comments during the analysis of the study.

8 Inverse Solution for Field Power Measurements

8.1 Summary

A method was successfully developed to identify cortical sources of incoherent fields of the human brain [45]. This makes it possible to locate cortical areas that participate in sensory and cognitive functions even when activity is not precisely time-locked to an external event, i.e., is voluntarily initiated. A unique mathematical solution to the inverse problem for field power provides a best estimate for distribution of average neuronal current power across the surface of cerebral cortex, as well as in specified subcortical areas.

8.2 Background

The extracranial spontaneous magnetic field of the human brain changes over time. Unlike the stationary fields of evoked brain responses, these fields cannot be sampled at different places at different times. However, other things being equal, field power averaged over time is stationary. Sources of these stationary field power patterns, and of changes of level within these patterns, can be identified. Changes in levels of this ongoing activity are related to cognitive processes, and also to pathology. We have developed a mathematically unique solution to this inverse problem given information as to the underlying cortical geometry. This permits the identification of regions involved in cognitive processes and those that reflect some pathological states.

An ostensible advantage of magnetic source imaging (MSI) is that it allows the use of simple models in locating sources of the brain's magnetic fields. At first such sources were modeled as current dipoles, although the actual generators of the fields are always extended regions of the cerebral cortex. Generally, such solutions to the inverse problem are not unique. Any number of intracranial sources could account for the same field patterns. However, as we demonstrated previously (Wang et al. [46] [47]), mathematically unique solutions to the inverse problem are possible, provided one has prior knowledge of the surfaces on which all sources may lie. This is a reasonable constraint since extracranial fields are largely due to intracellular ionic current flow normal to the surface of the cerebral cortex. Knowledge of cortical geometry can be obtained from high resolution MRI scans. This makes it possible to locate and delineate the shapes of patterns of current on the cortex. However, since field patterns cannot at present be measured over the entire scalp at one time, this approach is limited to sources whose field patterns are time-invariant. These stationary patterns can be discerned in the background noise of the brain through signal averaging even when measurements are made at different times. It is important to recognize that sources of stationary patterns are composed of synchronized current elements (Kaufman et al. [48]). However, the spontaneous activity of the brain does not produce a stationary field pattern. Although it is commonly treated as "noise", evidence is accumulating that it is locally modulated when subjects perform certain mental tasks.

The level of activity arising in different cortical areas is affected by sensory stimulation and also engagement in mental tasks. For example, when subjects search memory to determine if they had recently heard a tone or seen a visual form a short time ago, the ongoing activity detected over different portions of the scalp (Kaufman et al. [26] [49]) is suppressed during the search. This local modulation of spontaneous activity is highly correlated with the

time required to perform the task. Thus, local changes in cortical activity are analogous to changes in blood flow revealed by PET under similar circumstances, except that magnetic measurements also provide information on the time evolution. It is to be expected that similar though sustained differential levels of local activity accompany restricted blood supply to a region, or abnormal metabolic levels. Therefore, for clinical applications as well, it is of considerable importance to be able to localize and delineate these regional differences, both transient and sustained. The following sections of this report describe a method for identifying regions of the cortex whose level of incoherent activity is differentially affected by some task or state.

If the spontaneous fields due to incoherent activity are squared to obtain *field power*, then the averaged spatial pattern of power is determined by the underlying geometry of the source surface, as well as by average spatial nonuniformities in the amount of activity across the cortex (Wang et al. [47]). The relation between cortical structure and average field power pattern suggests that it is possible to locate and delineate differentially active regions of cortex, even when that activity is incoherent.

8.3 Theory

8.3.1 Inverse for Magnetic Field

Previously in dealing with measurements of magnetic field, the values of the field B_i measured normal to the observation surface by sensors placed at m positions were used to form a column vector $\mathbf{b}$ of m elements, each element being $\mathbf{b}_i = B_i$. We consider current sources within the cortex to be represented by a distribution across the cortex of n current dipoles Q_j with $j = 1, 2, \ldots n$, each oriented perpendicular to the cortical surface at its location. These values can also be represented as a vector $\mathbf{Q}$ of n elements, each element being $\mathbf{Q}_j = Q_j$. The field B_i measured by each sensor is described by a linear superposition of contributions from each of the Q_j. This linear relationship can be summarized by the following equation:

$$\mathbf{b} = \mathbf{LQ} \tag{1}$$

This is called the forward model for predicting the measured fields. The matrix $\mathbf{L}$ is called the *lead field matrix*. Its element L_{ij} describes the contribution of Q_j at position j on the cortex to the field B_i measured by sensor i. The inverse problem for field, which specifies the distribution of the sources from information on the measured fields, is obtained formally from Eq. 1 by multiplying both sides by the inverse of the lead-field matrix $\mathbf{L^{-1}}$:

$$\mathbf{L^{-1}b} = \mathbf{L^{-1}LQ} = \mathbf{Q} \tag{2}$$

In practice, the traditional inverse of the lead-field matrix does not exist, because it is not square ($m \neq n$). Moreover, it is ill-conditioned because of the presence of noise and measurement errors. However, we have shown how the Moore-Penrose inverse solution can be applied to this problem using computational techniques to obtain a mathematically unique solution based on the "Penrose inverse" $\mathbf{L^+}$ for the lead field matrix (Wang et al. [46]). Symbolically, the application of this approach is indicated by replacing the traditional inverse $\mathbf{L^{-1}}$ by the Penrose inverse $\mathbf{L^+}$:

$$\mathbf{L}^{+}\mathbf{b} = \mathbf{L}^{+}\mathbf{L}\hat{\mathbf{Q}} = \hat{\mathbf{Q}} \tag{3}$$

The solution $\hat{\mathbf{Q}}$ provides the best estimate for the image current in the least-squares sense, and the solution is the one with the minimum norm (minimum power) if more than one current configuration provides the same quality of fit to the data. That is why we call this solution the "minimum-norm least-squares inverse" (MNLS inverse). This has been applied successfully in many simulations to deduce the cortical current distrbution that accounts for a measured field pattern.

8.3.2 Inverse for Field Power

The problem at hand is to find an inverse solution from a measured field power pattern. Then the pattern of suppression of spontaneous activity across the cortical surface can determined. Do achieve this, we introduce a matrix $\mathbf{B}_p$ constructed from the vector $\mathbf{b}$ in the following way:

$$\mathbf{B}_p = \mathbf{b}\mathbf{b}^T \tag{4}$$

Its elements are $(\mathbf{B}_p)_{ij} = B_i B_j$, where $i, j = 1, 2, ..., m$. Therefore, the diagonal elements of $\mathbf{B}_p$ are the field power B_i^2, rather than field. This leads to a new linear model which relates field power to the source power rather than a linear relation (Eq. 1) between field *per se* and source strength. Thus,

$$\mathbf{B}_p = \mathbf{L}\mathbf{Q}_p\mathbf{L}^T \tag{5}$$

where $\mathbf{Q}_p$ is a matrix whose elements are products of source current at different locations: $(\mathbf{Q}_p)_{kl} = Q_k Q_l$ with $k, l = 1, 2, ..., n$. Therefore, the diagonal elements represent the distribution of source power. Note that Eq. 1 describing the relation between field and current has a matrix and two vectors, while Eq. 5 for the relation between field power and current power contains all matrices. We have developed a unique minimum-norm least-squares solution for the matrix equation expressed in Eq. 5. Thus, the best estimate for the image current power based on a measured field power distribution at a specified moment is given by

$$\mathbf{L}^{+}\mathbf{B}_p(\mathbf{L}^{+})^T = \hat{\mathbf{Q}}_p \tag{6}$$

Applying this equation makes it possible to delineate regions of cortex whose incoherent activity differs in power from that of its surrounding because of an ongoing cognitive process, or as a manifestation of a clinical disfunction, e.g., eschemia.

If we use $< >$ to denote the time average, and take the time average of the field power given by Eq. 6, we obtain

$$< \hat{\mathbf{Q}}_p >= \mathbf{L}^{+} < \mathbf{B}_p > (\mathbf{L}^{+})^T \tag{7}$$

where $< \mathbf{Q}_p >$ is the covariance matrix of image current, and $< \mathbf{B}_p >$ is the covariance matrix of measured fields. Note that the lead field matrix $\mathbf{L}$ is time invariant and so is its minimum-norm least-squares matrix $\mathbf{L}^{+}$, provided that the measures made at different times are made at the same positions.

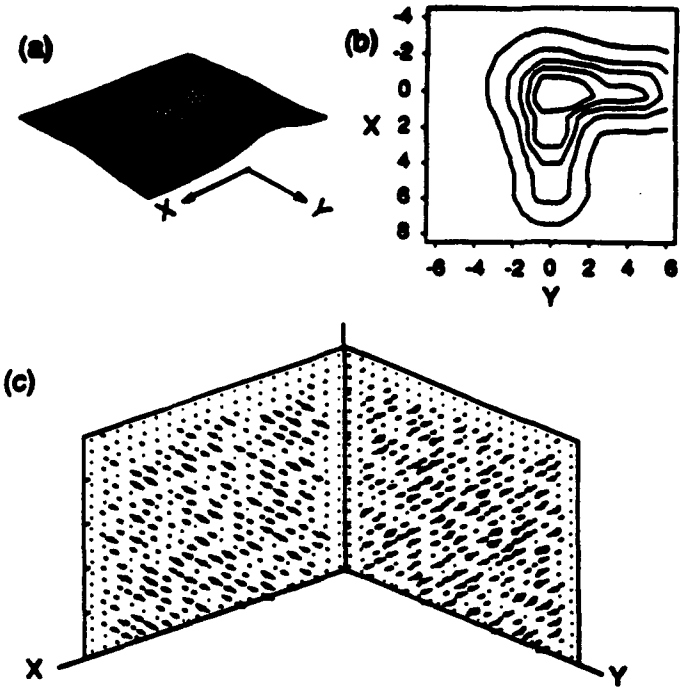

Figure 8: (a) 3-D plot of average field power across the observation plane from underlying spontaneous activity on the cortex forming the wall of a sulcus having a right-angle bend. The activity is represented by a random array of dipoles with strengths ranging from -1 to +1 computed for 100 independent random samples, one of which is illustrated in (c). (b) Contour plot of the average field power, whose two extensions lie above the walls of the source surface.

8.4 Simulations

An inverse solution for a set of time-averaged field power measurements can be represented by an array of dipoles whose time-averaged square moments are represented by the relative lengths of arrows or specified by the pattern of isocontours that describe the mean square moment density. Both of these can be referred to as the "image current power".

For purposes of illustration, surfaces representing the cerebral cortex are populated by a large number of current dipoles Q_j of random direction and magnitude. Each is perpendicular to the cortical surface at its location. Subsets of these elements are either incremented or decremented in magnitude, and the net fields of all of the elements are summed at the observation surface. In the simulation of the forward problem, the current dipole moments populating the source surface are sampled from a uniform distribution, and a new random seed is applied to the random number generator prior to the selection of any array. This assures an ever-changing field pattern at the observation surface. The fields recorded by the m detectors are used to construct the square matrix $\mathbf{B}_p$. One hundred such matrices (representing different time series) are averaged together to form the auro-correlation matrix. We then deduce the image of this source.

In these simulations the spontaneous activity is spread over the entire source surface (the L-shaped wall of Fig. 8). Each wall of the surface is assumed to be 5 cm × 5 cm. The randomized magnitudes and directions of current flow (to simulate background "noise"), are given values that range from $-1 \rightarrow +1$. Fig. 8c illustrates is one of the samples. Field values

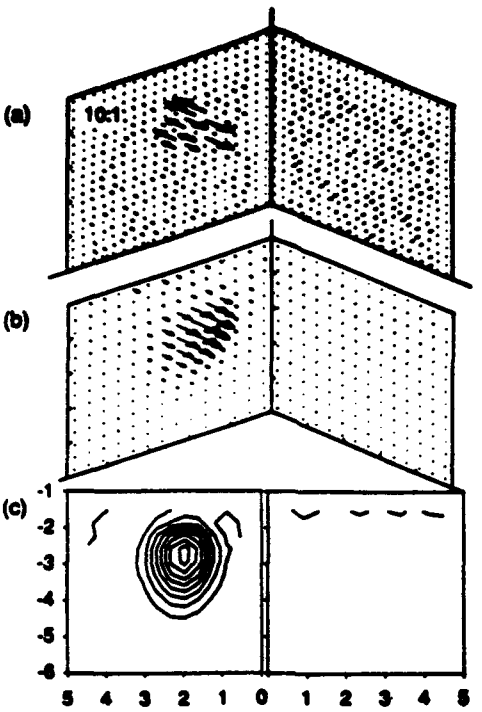

Figure 9: (a) Snapshot of dipoles having random strengths, with those in the center enhanced. The corresponding image current power (b) and (c) isopower density contours obtained from average over 100 samples of field power distributions.

are computed for each sensor, 1 cm apart on the 12 cm × 12 cm observation plane. The 100 plots of field power thus generated are averaged and illustrated by the L-shaped 3-D power plot in Fig. 8a and the contour plot in Fig. 8b. *It is of some interest to compare this plot* with one obtained with a cross-shaped sulcus rather than an L-shaped fold (Kaufman et al. [48]). This led to a power plot displaying 4 lobes. In general, the average field power plot is topologically related to the geometry of the underlying structure. Local departures from uniformity in average level of activity also affect the shape of the pattern (Kaufman et al. [48]). We now show that it is possible to form "images" of such regional inhomogeneities. The images are unique mathematical solutions to the inverse problem.

As our first example, we consider a uniform distribution of random activity across a surface, with a small circular region of 0.6 cm radius having its amplitude enhanced by a factor of 10. Fig. 9a shows one sample out of 100 su' ource distributions. Fig. 9b is a perspective view of the current power image derived from t. inverse. Because power is always positive, all of the arrows representing the incremented region point in the same direction, which is arbitrarily selected. However, the lengths of the arrows are proportional to the current dipole power. Fig. 9c is an isocontour plot representing the same inverse. Note that the contours surround the exact center of the original incremented current distribution of the source surface. Similar simulations were successfully carried out using multiple target areas, e.g., two on the same wall, or one on each of the two walls, and all were successfully recovered from the average field power patterns. Targets of different shape were also recovered and were recognizeable in the inverse power plots. The effects of increasing the source depth or reducing the signal-to-noise ratio degraded these images. However, the solutions were robust for noise levels below 15%.

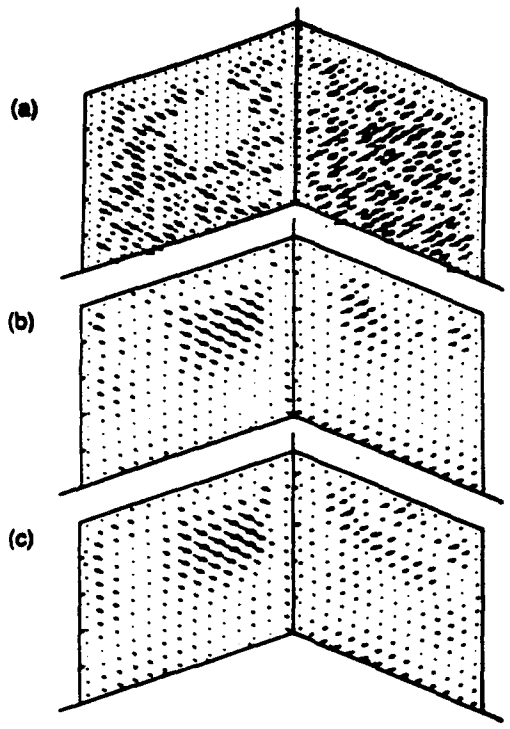

Figure 10: (a) Snapshot of dipoles having random strengths, with those in the center suppressed. The corresponding current power image (b) and (c) isopower density contours obtained from average over 100 samples of field power distributions.

It was equally feasible to recover targets produced by decrementing small region of each wall, where were otherwise uniformly active. This represents the important application for characterizing the distribution of neuronal sources that exhibit alpha suppression. An example is shown in Fig. 10. A circular target area of 1-cm radius is 10% of that of the surroundings. A single sample of a source distribution is shown in Fig. 10a. In this example, the power at each site for 100 such random samples with different initial seeds was computed and the average power for each site was computed. The image for average current power with target decremented was subtracted from the image for average baseline power (when not decremented). Fig. 10b and c show two such image power difference plots. The circular area of decremented power is clearly revealed.

Another interesting feature is also illustrated in Fig. 10b,c. Because different seeds defined the initial distribution of spontaneous activity for the baseline and decremented computations, there was not exact cancellation in areas where activity was not suppressed when the differences were computed. This residual appears as patches of image power difference that are not reproducible between subsequent averages, particularly as shown on the right wall of Fig. 10b,c. If the same seeds are used, these patches completely disappear and no activity is seen on the right wall. This simulation points out the requirement that samples must be obtained over an appropriately large number of events for representative characterizations of the mean power distribution to be obtained.

8.5 Conclusions

The main conclusion from this research is that it is possible to estimate mathematically unique inverse solutions to recover the location, shape and magnitude of a differentially active region of cortex, even when the activity is incoherent. This, together with earlier work, makes it possible to uniquely define both coherent and incoherent activity using maps of the extrancranial field and its power, together with MRI-based reconstructions of the individual person's brain. Therefore we can obtain accurate representations of cortical areas where spontaneous rhythms are suppressed when cognitive processes are being served. In this way the sequence of processing activity from one brain area to another can be followed. For instance, this approach can be applied to characterize an individual's strategies when mentally solving a problem, by determinig the sequence and timing of suppression over different areas of the brain.

While we have restricted our discussion to the brain's magnetic field, similar methods can applied to EEG data provided that anatomical and electrical properties are taken into account for the individual patient's skull, brain, and other tissues that affect the flow of volume currents.

9 Decay of Auditory Sensory Memory

9.1 Summary

Noninvasive magnetic source imaging (MSI) makes it possible to determine the lifetime of a memory trace established in human primary auditory cortex by the presentation of a tone. This lifetime predicts with high accuracy the duration of sensory memory for the loudness of the sound as determined by behavioral measures in individual subjects. This work will be reported as part of the Ph.D. Thesis submitted to the Department of Physics by Zhong-Lin Lü.

9.2 Background

It is well known that stimulation of human sense organs is initially represented for a brief period by a literal, labile, and modality specific neural copy. Neisser [50] coined the term *iconic memory* to stand for the initial representation of visual stimuli. Echoic memory is its counterpart for auditory stimulation. It is essential for integrating acoustic information presented sequentially over an appreciable period of time [51] [52] For example, speech perception is based on a continuous flow of words, spoken one after the other. Memory recall and recognition experiments suggest that the duration of short-term memory for sounds (of which speech is composed) lasts about 2 - 5 seconds [53] [54] [55] However, behavioral evidence for the putative echoic memories that make this kind of perception possible remains controversial [56]. Further, we lack physiological evidence for the precise location or locations of the neuronal substrate of this echoic memory in humans, e.g., whether it is peripherally or centrally located, or multiply represented in the nervous system. However, it is known that dichotic and binaural masking produce similar results, and this can only be explained by a central locus after binaural combination [57] [58]

The nature of loss (forgetting) of sensory memory is by no means clear. If the memory simply decays with time, the loss could be reflected by an increase in uncertainty of the comparison of recently heard memory items with a probe item. However, even this may be constrained by the possibility that subjects retain general information about the context, while they lose information about the specific item. Early in this century, Hollingworth [59] [60] discovered the central tendency of judgement: A subject's judgement of the magnitude of a stimulus lies near the middle of the range of stimuli employed in the experiment. The effect was also obtained by Hollingworth for hand movements and for perceived areas. Similar findings were found for lifted weights by Woodrow [61] and for sound intensities by Needham [62]. Helson [63] emphasized the role that the range of stimuli has on subsequent judgements of these stimuli or memories of them. However, our present behavioral findings establish a strong tendency for memory to regress toward the center of the range of previously heard sounds. Our evidence that the neuronal activation trace established in primary auditory cortex by a sound decays with the same lifetime provides direct support for the existence of a heirachical memory structure in which long-term and sensory memories interact with each other.

Experiments with animals (Weinberger et al. [64] [65]; Westenberg et al. [66]; Miller et al. [67]) suggest that the presence of a neuronal memory trace is indicated by a decrement in the level of the responses of single cells when a stimulus is presented repetitively. Advances

in magnetic source imaging (MSI) have made it possible to noninvasively determine the strength of neuronal activity in specific sensory regions within the human brain with high sensitivity and temporal resolution (Williamson et al. [68]). Using this technique, we have recently reported that neuronal responses to tone stimuli decay exponentially with time, and the lifetime in association cortex is several seconds longer than that in primary cortex in individual subjects (Lü et al. [69]). This confirms the idea that short-term memory is modality specific (Conrad [70]; Murdoch [71]). Further, the results are consistent with the conjecture of Kaufman *et al.* [29] that the N100 component of the event related potential or field may well play roles in echoic memory, while no evidence was found for a role of the source of this component in short-term memory scanning (working memory).

9.3 Method

Four right-handed adult volunteers (2 males and 2 females) served as subjects after providing informed consent. All of the studies were carried out within a magnetically shielded room which also provides a quiet environment. The subject sat comfortably with left and right index fingers resting on separate keys of a standard computer keyboard. Tone bursts of 200 ms duration, including 12 ms duration ramps at both onset and offset, were generated by an Amiga 1000 computer and presented monoaurally via earphones (Etymotic Research type ER3-5A earphones) and the acoustic environment were the same as used in the MSI studies on these subjects. One experimental session consists of 100 trials, with 5 s interval between the end of one trial and the beginning of the next. Each trial contains a test tone presented to one ear followed after a delay by a probe tone delivered to the other ear, with the delay randomly chosen with equal probabilities from 1, 2, 4, 6 and 8 s in one block, and 0.8, 1.5, 2.5, 3.5 and 5.3 s in another block. The intensity of the test tone was fixed at 85.3 dB (SPL) with its frequency randomly selected with equal probabilities from 800, 900 and 1100 Hz [1] The frequency of the probe tone was always the same as its corresponding test tone, and the ear of presentation for the test stimuli was fixed within each session but alternated across sessions. The task for the subject was a two alternative forced choice: press one key if the probe tone appeared louder than the test tone or the other key if it appeared softer. No immediate feedback was provided, but subjects were informed of the experimental results after the end of each session. A total of 6000 trials were collected for each subject. All the analyses were based on the data after excluding the first 20% of the trials of every session, since it was during this first set of presentations that the range of the loudness in the session established.

For each delay condition, a cumulative gaussian distribution was fit to the behavioral data after averaging the response scores for the loudness of each probe under a given delay condition. The subjective equal loudness point was defined as the mean of the gaussion distribution, and the uncertainty was estimated as the standard deviation of the distribution.

[1] Within each session, the intensity of the probe stimulus was randomly chosen with equal probabilities from one of two lists: (71.0, 74.5, 77.0, 78.9, 80.5, 81.8, 83.0, 84.0, 84.9, 85.8, 86.5, 87.2, 87.9, 88.5, 89.0, 89.5) or (83.0, 84.0, 84.9, 85.8, 86.5, 87.2, 87.9, 88.5, 89.0, 89.5, 90.0, 90.5, 91.0, 91.4, 91.8, 92.2, 92.5) db (SPL). The first list has a mean loudness that, together with the test stimulus, has a mean loudness that is 2.9 db lower than the loudness of the test tone, and the second list has a mean that is 2.5 db greater. Care was taken to ensure that the difference between the mean and test was sufficiently small that the subject could not judge which list was presented.

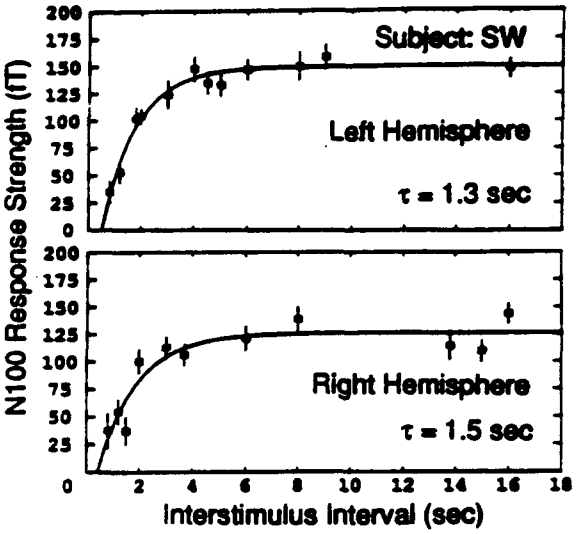

Figure 11: Peak magnetic field strength near the scalp approximately 100 ms following the onset of a tone burst stimulus (the "N100m" component) increases with interstimulus interval, as shown for measurements of activity in the left and right primary auditory cortices of a subject. Curves best fitting the data are associated with the indicated activation trace lifetimes.

Magnetic field recordings related to auditory evoked response were also collected for the subjects for whom there were no existing MSI data.

9.4 Neuromagnetic Data

Figure 11 illustrates the neuromagnetic data with which these psychophysical data were compared. It shows how the response strength of primary auditory cortex increases with the interstimulus interval (ISI) and approaches a maximum value for ISIs exceeding a few seconds.

In all cases, we find that such curves can be described adequately by the expression $A(1 - e^{(t-t_o)/\tau})$, where the amplitude A, lifetime τ, and time of decay onset t_o are fitting parameters.[2] We emphasize that the *shape* of the curve in each case is determined by a single parameter τ. The difference between the greater response strength obtained for very long ISIs and the value obtained at a given ISI is considered a measure of how much the activation trace diminished in strength since the preceding response. According to the relationship just given, the activation trace decays exponentially with time: $Ae^{-(t-t_o)/\tau}$. The onset of decay for the N100m component is at the onset of a tone and also at the offset of the tone. Thus

[2]The onset of decay, specified by the value of t_o commences at the offset of the preceding tone. As explained in [69], the N100m response to the offset of a tone is found to be habituated to the onset of the same tone, implying that the two activation traces have appreciable commonality. Thus an activation trace is established in primary auditory cortex by a tone burst stimulus expresses information that is contained within the early or late portions of the tone.

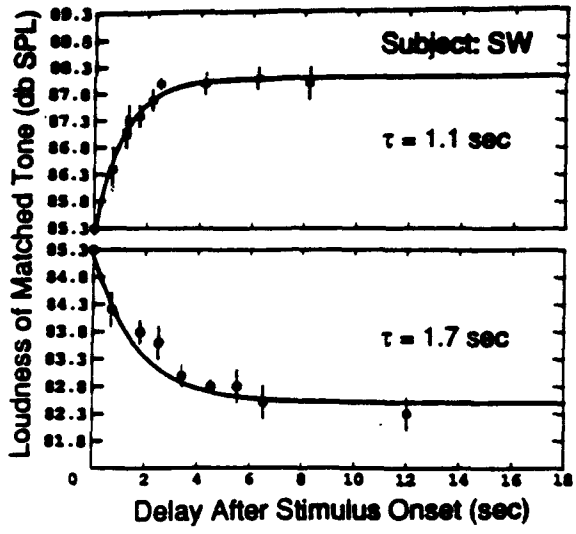

Figure 12: Remembered loudness of a tone determined by a forced choice match with probe tones presented at different delays following the test tone. Data represented by the closed squares were obtained when the mean loudness of the test and probe tones was 2.5 db greater than that of the test tone. Data represented by closed circles were obtained with the mean loudness 2.9 db lower. Error bars denote the standard deviation for each delay.

we conclude that both features share a largely common activation trace. For each subject, we reported [69] that the left and right hemisphere have essentially the same lifetimes for the N100m activation trace. Moreover, we also found that the lifetime of the activation trace for the the classic P180m component had essentially the same value as the N100m component for each individual subject. This suggests that the lifetime may well be characteristic of the cortical area, since neuronal sources for both N100m and P180m lie in the primary auditory cortex. In support of this suggestion, lifetimes for responses that arise in the association auditory cortex are found to be the same for each subject but are significantly longer than those of primary cortex.

9.5 Behavioral Studies

Behavior measures and the resulting psychometric functions enable us to test the hypothesis that echoic, or auditory sensory memory, is a direct reflection of the decay of the physiological activation trace in primary auditory cortex. As shown in Fig. 12, the subjective equal loudness match displays a strong dependence on delay since the test tone. In all cases it decays towards the middle loudness level of all probe and test stimuli. This suggests that though memory for specific features of acoustic stimuli is lost shortly after exposure, subjects may draw upon longer term global experience of ranges of stimului in making their judgements. This is true whether the mean loudness is greater or less than the loudness of the test tone. This shift is significantly greater than the uncertainties in the measurements. These results are consistent with the "central tendency" effects cited earlier and provide a neural modality-specific basis for such effects. As echoic memory decays, judgement is more heavily based toward the global patterns of recent experience and tends toward the middle

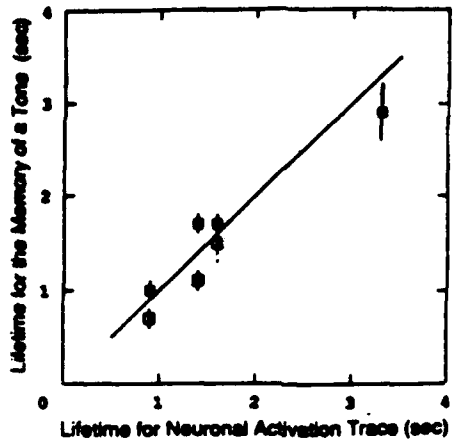

Figure 13: Agreement across four subjects between behavioral lifetimes for the decay of the loudness of a tone following its presentation and physiological lifetimes for the decay of the neuronal activation trace in primary auditory cortex. Open symbols denote behavioral lifetimes when the mean loudness of the probe tones is higher that of the test tones, and closed symbols denote the results when the mean loudness is lower.

magnitudes of the range of presented stimuli. As illustrated in Fig. 12 an exponential decay adequately describes this trend: $A + Be^{(} - t/\tau)$, where the amplitudes A and B and the lifetime τ are fitting parameters. In this way a unique lifetime can be defined for a subject's memory of the loudness of the sound.[3] Similar behavior has been observed for a total of 4 subjects whose individual memory lifetimes range from 0.8 to 3 sec. It is interesting that the loss of short-term sensory memory and the growing dominance of a longer term memory is not accompanied by a marked increase in the uncertainly for the loudness of the probe that best matches the test for a given delay.

9.6 Comparison Between Cortical and Behavioral Lifetimes

The correspondance between the physiological lifetime obtained from the decay of the activation trace of N100m and the behavioral lifetime for loudness of the sound is quite accurate across subjects, as illustrated in Fig. 13. The excellent agreement suggests a causal relationship between the decay of the memory trace and the evolution of the perception.

These results suggest that noninvasive measurements of cortical activation lifetimes may provide an objective and meaningful characterization of sensory memory lifetimes for individual subjects. This was achieved in the present study by exploiting an advantage in MSI whereby the precise location and orientation of the neuronal source current can be established, so that its field pattern can be predicted. This information identified locations over the scalp where the magnetic field of only that particular source was appreciable. Another feature of this technique is its rapid time response, which permits changes over fractions of a second to be well characterized. The present study suggests that extensions of these pro-

[3]Because the overall change in loudness was kept relatively small, if there were an exponential decay it would have the same exponent whether loudness is expressed in terms of the power amplitude, pressure amplitude, or logarithm of the power amplitude (in decibels).

cedures may be capable of characterizing a variety of memory functions that are supported by cortical areas of other sensory modalities.

References

[1] R.N. Shepard. The mental image. *American Psychologist*, 33:125–137, 1978.

[2] F. Golla, E. L. Hutton, and W. G. Walter. The objective study of mental imagery. I. Physiological concomitants. *J. Mental Sci.*, 75:216–223, 1943.

[3] R. N. Shepard and J. Meltzer. Mental rotation of three-dimensional objects. *Science*, 171:632–634, 1971.

[4] R. N. Shepard and L. A. Cooper. *Mental Images and their Transformations.* MIT Press, Cambridge, 1982.

[5] S. N. Kosslyn. *Ghosts in the Mind's Machine.* Norton, New York, 1983.

[6] M.J. Farah. The neurological basis of mental imagery: A componential analysis. *Cognition*, 18:245–272, 1984.

[7] J.R. Anderson. *Cognitive Psychology and its Implications.* W.H. Freeman & Company, New York, 2nd edition, 1985.

[8] L.A. Cooper and R.N. Shepard. Chronometric studies of the rotation of mental images. In W.G. Chase, editor, *Visual information processing.* Academic Press, New York, 1973.

[9] R.A. Finke and R.N. Shepard. Visual functions of mental imagery. In K.R. Boff, L. Kaufman, and J.P. Thomas, editors, *Handbook of Perception and Human Performance: Vol. II, Cognitive Processes and Performance*, chapter 37, pages 1–55. John Wiley and Sons, New York, 1986.

[10] Z. W. Pylyshyn. The imagery debate: Analogue media versus tacit knowledge. *Psych. Rev.*, 88:16–45, 1981.

[11] M. J. Farah. Is visual imagery really visual? Overlooked evidence from neuropsychology. *Psych. Rev.*, 95:307–317, 1988.

[12] M. Farah, F. Peronnet, L.L. Weisberg, and F. Perrin. Electrophysiological evidence for shared representational medium for visual images and visual percepts. *J. Exp. Psych.*, 117:248–257, 1988.

[13] G. R. Mangun and S. A. Hillyard. Spatial gradients of visual attention: Behavioral and electrophysiological evidence. *Electroenceph. clin. Electrophysiol.*, 70:417–428, 1988.

[14] F. Peronnet and M.J. Farah. Mental rotation: An event-related potential study with a validated mental rotation task. *Brain and Cog.*, 9:279–288, 1989.

[15] D.S. Ruchkin, R. Johnson, H. Canoune, and W. Ritter. Event-related potentials during arithmetic and mental rotation. *Electroenceph. Clin. Neurophysiol.*, 79:472–487, 1991.

[16] H. Berger. Uber das Elektroenkephalogramm des Menschen. II. *J. Psychol. Neurol. (Lpz.)*, 40:160–179, 1930.

[17] L. Kaufman and Y. Locker. Sensory modulation of the EEG. *Proc. Amer. Psychology Assoc.*, pages 179–180, 1970.

[18] G. Pfurtscheller. Event-related desynchronization mapping: Visualization of cortical activation patterns. In F.H. Duffy, editor, *Topographic Mapping of Brain Electrical Activity*, pages 99–111. Butterworth, Stoneham, 1986.

[19] D. Lehmann. EEG, evoked potentials, and eye movements. In P. Bach-y-Rita and C.C. Collins, editors, *The Control of Eye Movements*, pages 141–173. Academic Press, London, 1971.

[20] H.H. Jasper and H.L. Andrews. Electro-encephalography. III. Normal differentiations of occipital and precentral regions in man. *Arch. Neurol. Psychiat.*, 39:96–115, 1938.

[21] G. Pfurtscheller. Central beta rhythm during sensory motor activities in man. *Electroenceph. clin. Neurophysiol.*, 51:253–264, 1981.

[22] G. Pfurtscheller and A. Aranibar. Evaluation of event-related desynchronization (ERD) preceding and following voluntary self-paced movement. *Electroenceph. clin. Neurophysiol.*, 46:138–146, 1979.

[23] G. Pfurtscheller and W. Klimesch. Event-related desynchronization during motor behavior and visual information processing. In C.H.M. Brunia, G. Mulder, and M. Verbaten, editors, *Event-Related Brain Research, Electroencephalography and Clinical Neurophysiology*, volume suppl. 42, page in press. Elsevier, Amsterdam, 1991.

[24] W. Klimesch, G. Pfurtscheller, and H. Schimke. Pre- and poststimulus processes in category judgement tasks as measured by event-related desynchronization (ERD). *J. Psychophysiol.*, page in press, 1991.

[25] L. Kaufman, M. Glanzer, Y. M. Cycowicz, and S. J. Williamson. Visualizing and rhyming cause differences in alpha suppression. In S. J. Williamson, M. Hoke, G. Stroink, and M. Kotani, editors, *Advances in Biomagnetism*, pages 241–244, New York, 1989. Plenum.

[26] L. Kaufman, B. Schwartz, C. Salustri, and S.J. Williamson. Modulation of spontaneous brain activity during mental imagery. *J. Cog. Neurosci.*, 2:124–132, 1990.

[27] S. J. Williamson, J.-Z. Wang, and R. J. Ilmoniemi. Method for locating sources of human alpha activity. In S. J. Williamson, M. Hoke, G. Stroink, and M. Kotani, editors, *Advances in Biomagnetism*, pages 257–260, New York, 1989. Plenum.

[28] S.J. Williamson and L. Kaufman. Advances in neuromagnetic instrumentation and studies of spontaneous brain activity. *Brain Topography*, 2:129–139, 1989.

[29] L. Kaufman, S. Curtis, J.-Z. Wang, and S.J. Williamson. Changes in cortical activity when subjects scan memory for tones. In *8th International Conference on Biomagnetism*, page in press. Münster, Germany, 1991.

[30] J. Tiihonen, R. Hari, M. Kajola, J. Karhu, S. Ahlfors, and S. Tissari. Magnetoencephalographic 10-hz rhythm from the human auditory cortex. *Neurosci. Lett.*, pages 303–305, 1991.

[31] S. J. Williamson and L. Kaufman. Analysis of neuromagnetic signals. In A. S. Gevins and A. Rémond, editors, *Methods of Analysis of Brain Electrical and Magnetic Signals*, volume 1 of *Handbook of Electroencephalography and Clinical Neurophysiology, Revised Series*, chapter 14, pages 405–448. Elsevier, Amsterdam, 1987.

[32] D. Lehmann and W. Skrandies. Reference-free identification of components of checkerboard-evoked multichannel potential fields. *Electroenceph. Clin. Neurophysiol.*, 48:609–621, 1980.

[33] S. J. Williamson, M. Pelizzone, Y. Okada, L. Kaufman, D. B. Crum, and J. R. Marsden. Magnetoencephalography with an array of SQUID sensors. In H. Collan, P. Berglund, and M. Krusius, editors, *ICEC10: Proc. Tenth International Cryogenic Engineering Conference*, pages 339–348. Butterworth, Guildford, England, 1984.

[34] T. Yamamoto, S. J. Williamson, L. Kaufman, C. Nicholson, and R. Llinás. Magnetic localization of neuronal activity in the human brain. *Proc. Natl. Acad. Sci. USA*, 85:8732–8736, 1988.

[35] D. Lehmann. *Principles of Spatial Analysis*, volume 1 of *Handbook of Electroencephalography and Clinical Neurophysiology, Rev. Ser.*, pages 309–354. Elsevier, Amsterdam, 1987.

[36] C. M. Michel, D. Lehmann, B. Henggeler, and D. Brandeis. Localization of the sources of EEG delta, theta, alpha and beta bands using the FFT dipole approximation. *Electroenceph. Clin. Neurophysiol.*, page in press, 1992.

[37] L. K. Morrell. Some characteristics of stimulus-provoked alpha-activity. *Electroenceph. Clin. Neurophysiol.*, 21:552–561, 1966.

[38] R. J. Ilmoniemi, S. J. Williamson, and W. E. Hostetler. New method for the study of spontaneous brain activity. In K. Atsumi, M. Kotani, S. Ueno, T. Katila, and S. J. Williamson, editors, *Biomagnetism '87*, pages 182–185, Tokyo, 1988. Tokyo Denki University Press.

[39] D. Lehmann, H. Ozaki, and I. Pal. EEG alpha map series: Brain micro-states by space-oriented adaptive segmentation. *Electroenceph. Clin. Neurophysiol.*, 67:271–288, 1987.

[40] S.M. Kosslyn, J. Brunn, K.R. Cave, and R.W. Wallach. Differences in mental imagery ability: A computational analysis. *Cognition*, 18:195–243, 1984.

[41] A. C. Papanicolaou, G. Deutsch, W. T. Bourbon, K. W. Will, D. W. Loring, and H. M. Eisenberg. Convergent evoked potential and cerebral blood flow evidence of task-specific hemispheric differences. *Electroenceph. Clin. Neurophysiol.*, 66:515–520, 1987.

[42] M.C. Corballis and J. Sergent. Hemispheric specialization for mental rotation. *Cortex*, 25:15–25, 1989.

[43] M.C. Corballis and J. Sergent. Mental rotation in a commissurotomized subject. *Neuropsychologia*, 27:585–597, 1989.

[44] P. Servos and M. Peters. A clear left hemisphere advantage for visuo-spatially based verbal categorization. *Neuropsychologia*, 28:1251–1260, 1990.

[45] J.-Z. Wang, L. Kaufman, and S.J. Williamson. Imaging regional changes in the spontaneous activity of the brain: An extension of the unique minimum-norm least-squares estimate. *Electroenceph. Clin. Neurophysiol.*, page in press, 1992.

[46] J.-Z. Wang, S.J. Williamson, and L. Kaufman. Magnetic source images determined by a lead-field analysis: The unique minimum-norm least-squares estimation. *IEEE Trans. Biomed. Engr.*, 39:665–675, 1992.

[47] J.-Z. Wang, L. Kaufman, and S.J. Williamson. A unique inverse estimate of magnetic source images: The minimun-norm least-squares approach. In *17th Intl. Conf of IEEE EMBS meeting, Paris, 1992, in press.*, 1992.

[48] L. Kaufman, J. Kaufman, and J.Z. Wang. On cortical folds and neuromagnetic fields. *Electroenceph. Clin. Neurophysiol.*, 79:211–226, 1991.

[49] L. Kaufman, S. Curtis, J.-Z. Wang, and S.J. Williamson. Changes in cortical activity when subjects scan memory for tones. *Electroenceph. Clin. Neurophysiol.*, 82:266–284, 1991.

[50] U. Neisser. *Cognitive Psychology.* Appleton-Century-Crofts, New York, 1967.

[51] R.G. Crowder. *Principles of Learning and Memory.* Academic Press, New York, 1976.

[52] D. W. Massaro. *Experimental Psychology and Information Processing.* U. Chicago Press, Chicago, 1975.

[53] M. Glanzer and A.R. Cunitz. Two storage mechanisms in free recall. *J. Verbal Learning and Verbal Behavior*, 5:351–360, 1966.

[54] A. M. Treisman. Selective attention in man. *Brit. Med. Bull.*, 20:12–16, 1964.

[55] W.A. Wickelgren. Auditory or articulatory coding in verbal short-term memory. *Psychol. Rev.*, 76:232–235, 1969.

[56] R. G. Crowder. Sensory memory systems. In E. C. Canderette and M. P. Friedman, editors, *Handbook of Perception*, volume VIII, chapter 10, pages 343–373. Academic Press, New York, 1978.

[57] D. W. Massaro. Retroactive interference in short-term recognition memory for pitch. *J. Exp. Psych.*, 83:32–39, 1970.

[58] D. B. Pisoni. Auditory and phonetic memory codes in the discrimination of consonants and vowels. *Percep. and Psychophys.*, 13:253–260, 1973.

[59] H.L. Hollingworth. *Arch. Psych.*, 13, 1909.

[60] H.L. Hollingworth. *J. Philos.*, 7:461–469, 1910.

[61] H. Woodrow. *Am. J. Psychol.*, 45:391, 1933.

[62] J.G. Needham. *J. Exp. Psych.*, 18:530–543, 1935.

[63] H. Helson and E.V. Fehrer. *Am. J. Psych.*, 44:79–102, 1964.

[64] N.M. Weinberger and D.M. Diamond. Physiological plasticity in auditory cortex: Rapid induction by learning. *Progress in Neurobiology*, 29:1–55, 1987.

[65] N.M. Weinberger, J.H. Ashe, R. Metherate, T.M. McKenna, D.M. Diamond, and J. Bakin. Retuning auditory cortex by learning: A preliminary model of receptive field plasticity. *Concepts in Neurosci.*, 1:91–132, 1990.

[66] I. S. Westenberg, G. Paige, B. Golub, and N. M. Weinberger. Evoked potential decrements in auditory cortex. I. Discrete-trial and continual stimulation. *Electroenceph. Clin. Neurophysiol.*, 40:337–355, 1976.

[67] E.K. Miller, L. Li, and R. Desimone. A neural mechanism for working and recognition memory in inferior temporal cortex. *Science*, 254:1377–1379, 1991.

[68] S.J. Williamson and L. Kaufman. Neuromagnetic studies of sensory functions and mental imagery. In C.H.M. Brunia, G. Mulder, and M. Verbaten, editors, *Event-Related Brain Research*, chapter Suppl. 42, page in press. Elsevier, Amsterdam, 1991.

[69] Z.-L. Lũ, S.J. Williamson, and L. Kaufman. Human auditory primary and association cortex have differing lifetimes for activation traces. *Brain Res.*, 527:236–241, 1992.

[70] R. Conrad. Acoustic confusions in immediate memory. *Brit. J. Psychol.*, 55:75–84, 1964.

[71] B. B. Murdoch, Jr. and K. D. Walker. Modality effects in free recall. *Verbal Lrng. and Verbal Beh.*, 86:665–676, 1969.